NUMERICAL SOLUTION METHODS FOR BOUNDARY VALUE PROBLEMS FOR THE LAPLACE EQUATION IN SEMI-INFINITE DOMAINS

**A Thesis Submitted to
the Graduate School of
İzmir Institute of Technology
in Partial Fulfillment of the Requirements for the Degree of**

MASTER OF SCIENCE

in Mathematics

**by
Sabahat Defne Plattürk**

**June 2023
İZMİR**

We approve the thesis of **Sabahat Defne Plattürk**

Examining Committee Members:

_____
Prof. Dr. Gamze TANOĞLU
Department of Mathematics, İzmir Institute of Technology

_____
Assoc. Dr. Nasser AGHAZADEH
Department of Mathematics, İzmir Institute of Technology

_____
Asst. Dr. Demet ERSOY ÖZDEK
Department of Mathematics, İzmir University of Economics

22 June 2023

_____
Prof. Dr. Gamze TANOĞLU
Supervisor, Department of Mathematics
İzmir Institute of Technology

_____   _____
Prof. Dr. Şirin Atılgan BÜYÜKAŞIK   **Prof. Dr. Mehtap EANES**
Head of the Department of   Dean of the Graduate School
Mathematics

ACKNOWLEDGMENTS

ABSTRACT

NUMERICAL SOLUTION METHODS FOR BOUNDARY VALUE PROBLEMS FOR THE LAPLACE EQUATION IN SEMI-INFINITE DOMAINS

The essential purpose of this thesis is to get numerical solutions of the Laplace Equation Boundary Value Problems subject to Dirichlet and Mixed boundary conditions on doubly connected semi-infinite domains, namely the upper half plane and semi-infinite strips, using boundary integral equations. Conformal maps served as a tool to transform the doubly connected semi-infinite domains into a doubly connected bounded domain. Images of boundary conditions are evaluated and the accuracy of the conformal maps are investigated. Then each problem is reduced to a system of linear boundary integral equations by representing the solution to the boundary value problems as combinations of double- and single-layer potentials. In the case of Dirichlet boundary conditions, we used a modification that ensures the unique solvability of the system of Fredholm Integral Equations of the second kind. However, in the case of mixed boundary conditions, such a modification is not needed. After the investigations of uniqueness and existence of solutions to the constructed systems of integral equations of the second kind, the systems of equations are solved by using the Nyström method, based on quadrature rules. For the numerical integration of integral operators with continuous kernels, the trapezoidal rule is used. For the numerical integration of the kernels with logarithmic singularity, we first split off the singularity and apply an extremely accurate quadrature rule for the improper integrals. Error analysis for both numerical integration techniques are given in details and the accuracy of Nyström Method which depend on the quadrature method is explained. Different test cases are considered to check the accuracy of the method and the order of convergence and error results are illustrated by numerical examples.

ÖZET

YARI SONSUZ ALANLARDA LAPLACE DENKLEMİ İÇİN SINIR DEĞER PROBLEMLERİNİN SAYISAL ÇÖZÜM YÖNTEMLERİ

Bu tezin temel amacı çift bağlantılı yarı-sonsuz alanlarda Dirichlet veya Karışık sınır değerleri ile tanımlanmış Laplace denklemi için sınır değer problemlerinin sayısal çözümlerini bulmaktır. Açıkorur dönüşümler yardımı ile çift bağlantılı yarı-sonsuz alanlar, çift bağlantılı sonlu alanlara dönüştürülmüştür. Dönüşümlerin bileşke fonksiyon olduğu durumlarda doğrulukları kontrol edilmiş ve hatalar düzeltilmiştir. Daha sonra problemler, tek- ve çift-katman potansiyelleri kullanılarak, doğrusal sınır integral denklem sistemi şeklinde yazılmıştır. Dirichlet sınır değerler problemlerinde İkinci Tür Fredholm Integral Denklem Sisteminin çözümünün özgünlüğünü garanti eden bir modifikasyon kullanılmıştır. Buna karşın, karışık sınır değer problemlerinde bu modifikasyona gerek duyulmaksızın çözümün özgünlüğü kanıtlanabilmiştir. çözümlerin özgünlüğünün araştırıl-masından sonra bu integral denklem sistemleri Nyström Yöntemi kullanılarak sayısal olarak çözülmüştür. Sayısal integral alma yöntemi olarak sürekli kerneli olan integral operatörlerini hesaplamak için yamuk kuralı kullanılırken, zayıf tekil kerneli olan integral operatörlerini hesaplamak için ise logaritmik tekillik kernelden ayrılıp bir kısım analitik olarak hesaplanırken diğer kısım has olmayan integrallere özgü bir sayısal integral alma yöntemi ile hesaplanmıştır. İki sayısal integral alma yöntemi için de hata analizleri yapılmış ve Nyström Yönteminin doğruluğu açıklanmıştır. Farklı senaryolar ile yöntemin doğruluğu test edilmiş olup hata sonuçları sayısal örnekler ile görselleştirilmiştir.

TABLE OF CONTENTS

LIST OF FIGURES

LIST OF TABLES

CHAPTER 1

INTRODUCTION

Partial differential equations give us a language for writing down what we observe in the real world, and Laplace Equation is one of the most useful partial differential equation. The theory of solutions of the Laplace equation is called potential theory and the solutions of it are called harmonic functions. The Laplace equation occurs in various fields of science and engineering. It is essential to understanding a variety of scientific processes, including heat conduction, gravitation [1], electrostatics [2], [3], fluid movement [4], description of waves [5], [6], as it represents the steady-state behavior of scalar fields. For complicated geometries and boundary conditions, it is often difficult or even impossible to solve the Laplace equation analytically. In these kinds of situations, numerical approaches offer an effective way to arrive at approximations of solutions and get a deep understanding of the underlying physical processes [7], [8].

This thesis focuses on Boundary Value Problems for Laplace Equation in different semi-infinite domains subject to two different types of boundary conditions. The first one is the Dirichlet Problem which is a special situation in electric impedance tomography, for more details see [9], [10] and the second problem we discuss is a Mixed Boundary Value Problem, see [11]. We propose methods to solve those boundary value problems in doubly connected semi-infinite domains. Our first domain is the upper half plane with a peanut-shaped hole, the other domains we consider are horizontal and vertical strips with again a peanut-shaped hole.

1.1. Problem description

Let $D_1 \subset \mathbb{R}^2$ be a canonical semi-infinite domain such as a half plane, a strip, a half strip or a quadrant with boundary Γ_1, $D_0 \subset \mathbb{R}^2$ be a bounded and simply connected domain with boundary Γ_0 of class C^2 such that $\bar{D}_0 \subset D_1$, and $D = D_1 \backslash \bar{D}_0$, $\partial D = \Gamma_0 \cup \Gamma_1$ where $\Gamma_0 \cap \Gamma_1 = \emptyset$.

Given a function $f \in C(\Gamma_1)$, the aim is to find bounded solutions $u \in C^2(D)$ to the

Laplace Equation

$$\Delta u = 0 \text{ in } D \tag{1.1}$$

which satisfies the Dirichlet or Mixed boundary conditions respectively,

$$u = f \text{ on } \Gamma_0, \ u = g \text{ on } \Gamma_1 \tag{1.2}$$

or

$$\frac{\partial u}{\partial \nu} = f \text{ on } \Gamma_0, \ u = g \text{ on } \Gamma_1 \tag{1.3}$$

We know that both Dirichlet and Mixed problems has unique solution [9],[12].

These problems can also be solved by using Green's Function Technique, but it has some disadvantages compared to our method.

1.2. Outline of Thesis

The following is the structure of the thesis outline;

Chapter 2 basically explains the process of mapping from doubly connected semi-infinite domains to the unit circle. Besides, this chapter includes calculations for images of the boundary conditions.

Chapter 3 contains fundamental definitions and theorems of potential theory. This chapter also includes Green's Theorems and Green's Function Technique to solve the boundary value problems.

Then using the definitions and theorems from Chapter 3, Chapter 4 introduces the representations of the solutions to the problems by using single- and double layer potentials. This chapter proves the existence and uniqueness of solutions to the problems.

Chapter 5 deals with the numerical solutions of Boundary Integral Equations represented in Chapter 4. For the Integral Equations with continuous kernels Nyström Method based on Trapezoidal Rule is used to approximate, while for the weakly singular kernels a special quadrature formula is used. Also, error analysis for the quadrature methods is contained in this chapter.

Chapter 6 contains the test cases and numerical examples for the numerical method constructed in Chapter 5.

Chapter 7 analyzes the results and briefly introduces the conclusions of this thesis.

CHAPTER 2

CONFORMAL MAPPING

This chapter delves into the fascinating field of mapping semi-infinite domains to the unit circle using compositions of conformal mappings. This subject lies at the intersection of complex analysis and geometric transformations. We thoroughly examine the accuracy and applicability of these transformations in real-life situations, ensuring their reliability and robustness. Furthermore, the insights and outcomes obtained from this chapter will serve as fundamental tools in Chapter 6.

Theorem 2.1 (Riemann Mapping Theorem) *If $\Omega \subset \mathbb{C}$ is any simply connected open subset, not equal to the entire complex plane, then there exists a one-to-one complex analytic map $\omega = g(z)$, satisfying the conformality condition $g'(z) \neq 0$ for all $z \in \Omega$, that maps Ω to the unit disk $D = \{|\omega| < 1\}$.*

Through its impressive achievements, the Riemann mapping theorem enables us to understand conformal mappings from semi-infinite domains onto the unit circle. With its critical role in complex analysis, this significant theorem proves that there is always a unique conformal map between all semi-infinite domains and the unit circle, except the whole plane.

2.1. Transformation of Upper Half Plane

We start with constructing the transformation for the domain given in figure 2.1.
We need to find a formula, namely ω, that maps the upper half plane to the unit circle.
The points $0, 1, \infty$ should be mapped to $1, i, -1$ respectively. Let

$$\omega(z) = \frac{az + b}{cz + d}, \tag{2.1}$$

be a Möbius Transformation. We can find a, b, c, d with some algebraic calculations. Since $\omega(\infty) \neq \infty$, $c \neq 0$, Let us assume $c = 1$. Then since $\omega(\infty) = -1$, that is $a = -1$. We have $\omega(z) = \frac{-z+b}{z+d}$, and $\omega(0) = 1$, implies that $b = d$. Then since $\omega(1) = i$ we have
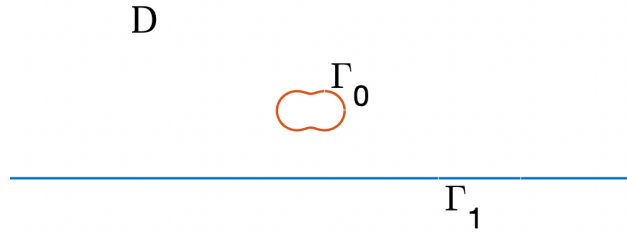
Figure 2.1. Original Domain

$b = d = i$.

Hence, we have $\omega(z)$ that maps the upper half plane to the unit circle:

$$\omega(z) = \frac{-z + i}{z + i} \tag{2.2}$$

Definition 2.1 *The conformal map* (2.2) *is bijective with its analytic inverse,*

$$z = \frac{i - i\omega}{1 + \omega}. \tag{2.3}$$

The inverses of the conformal maps are straightforward. For the proof of bijectivity, we refer to [13].

Since the upper half plane is transformed to the unit circle, we need to find the image of Γ_0 inside the transformed region. We consider Γ_0 as,

$$\Gamma_0 := \{z(t) = (r(t) \cos t, r(t) \sin t + 2),\ t \in [0, 2\pi]\} \tag{2.4}$$

where $r(t) = \sqrt{\cos^2 t + 0.25 \sin^2 t}$. Then we substitute the equation of Γ_0 directly to (2.2). Then we have the final version of our transformed domain.
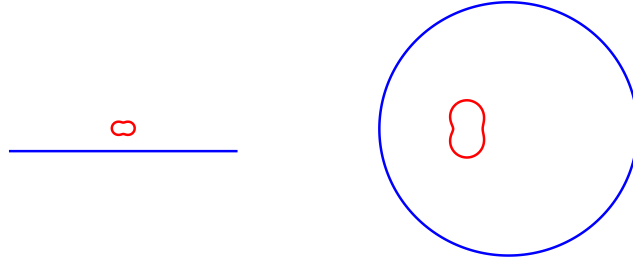
Figure 2.2. Visualization of the Transformation (2.2)

2.2. Transformation of Semi-infinite Strips

In this section, we map semi-infinite strips to the unit circle. To that end, we use compositions of conformal mappings. Where we use conformal maps derived by using Schwarz-Christoffel Transformation and Möbius Transformations. Besides, we investigate the reliability of the transformations.

2.2.1. Semi-infinite Horizontal Strip

Let the semi-infinite horizontal strip be defined as $\Gamma_1 := \{(x, y) : -\infty \leq x \leq \infty, -\pi/2 \leq y \leq \pi/2\}$. We know that the map $\gamma(z) = e^z$, it maps Γ_1 to the right half plane, see [14]. Also, by following the same process of previous section, we can construct the map that sends the right half plane to the unit circle, that is

$$\xi = \frac{\omega - 1}{\omega + 1}$$

We may compose γ and ξ, because composition of two differentiable functions is differentiable, to find the map that transforms the strip Γ_1 to the unit circle. And let $\sigma(z)$ be the transformation formula, it will look like,

$$\sigma(z) = \xi \circ \gamma(z) = \frac{e^z - 1}{e^z + 1} \tag{2.5}$$

The conformal mapping (2.5) maps the semi-infinite horizontal strip to the unit circle obviously, but many numerical errors could occur due to round-off errors while we are transforming the semi-infinite horizontal strip to the right half plane. Therefore we need to be careful while we are mapping the strip (figure 2.5, left). To this end, we will apply the conformal maps γ and ξ separately. In figure 2.3, you may see the visualization of the map γ.
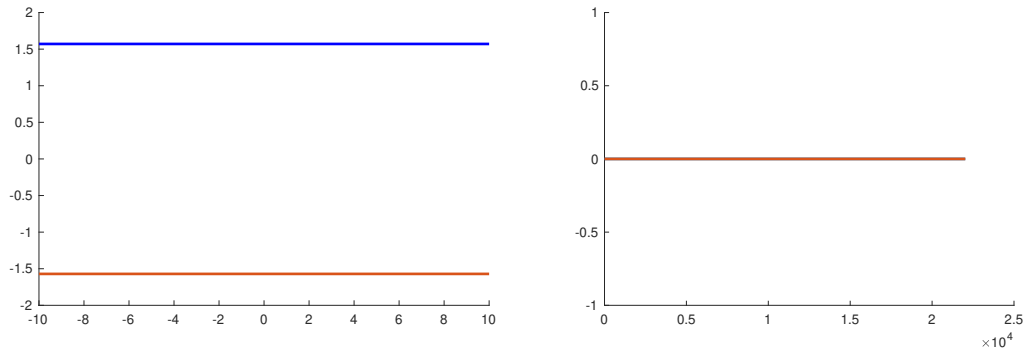
Figure 2.3. Visualization of the conformal map γ before treatment

In figure (2.3), we see that a huge error occurred during conformal mapping. Two boundaries of the horizontal strip are transformed to a single line (we cannot see the blue line because it is behind the red line) in the mapped domain. To avoid this situation, we need to treat the lines of the strip separately. We first recall our strip, $\Gamma_1 = \{(x, y) : -\infty \leq x \leq \infty, -\pi/2 \leq y \leq \pi/2\}$. We have two infinite boundaries, one is $y = -\pi/2$ and the other one is $y = \pi/2$. We recall our conformal map γ and ξ by using Euler's Formula we rewrite it as follows,

$$e^z = e^{x+iy}$$
$$= e^x(\cos y + i \sin y).$$

Now, we substitute y values of the lines and define the maps separately. For the boundary $y = -\pi/2$, we have $\gamma = -ie^x$, and for the boundary $y = \pi/2$, we get $\gamma = ie^x$. It can be understood from figure 2.4, our map is more reliable after treatment.
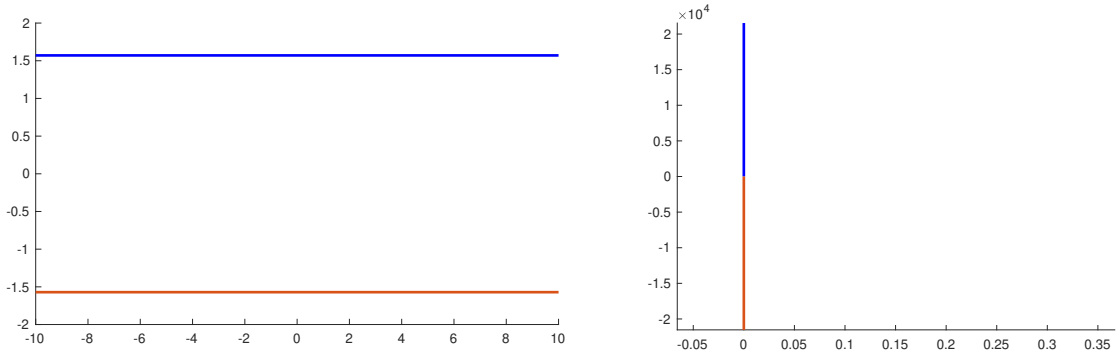
Figure 2.4. Visualization of the conformal map γ after treatment

Definition 2.2 *Inverse of the conformal map* (2.5) *can be found as,*

$$z = \ln -\frac{1+\sigma}{\sigma-1}. \tag{2.6}$$

This time, we consider Γ_0 as

$$\Gamma_0 := \{z(t) = (r(t)\cos t, r(t)\sin t),\, t \in [0, 2\pi]\}$$

where $r(t) = \sqrt{\cos^2 t + 0.25 \sin^2 t}$. We find the image by putting the equation of Γ_0 to the map (2.5). Visualization of the transformation is given in the figure 2.5.
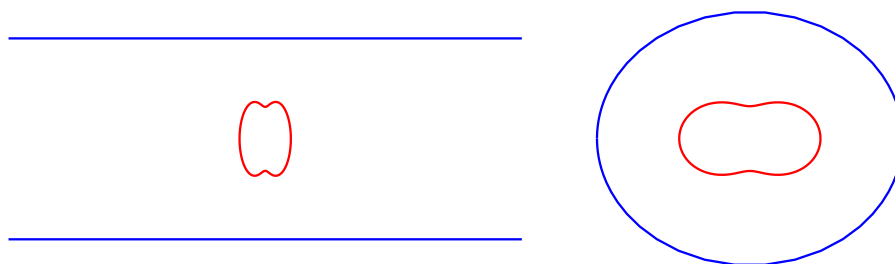
Figure 2.5. Visualization of the Transformation (2.5)

7

2.2.2. Semi-infinite Horizontal Half-Strip

Another interesting example of semi-infinite domains is the semi-infinite horizontal half-strip. Let our semi-infinite horizontal half-strip be defined as $\Gamma_1 := \{(x, y) : 0 \leq x \leq \infty, 0 \leq y \leq \pi\}$. We know that $\mu(z) = \cosh z$ transforms the semi-infinite half strip to the upper half plane, see [15]. Then by using the conformal map (2.2) we transform the upper half-plane to the unit circle. Composing the maps gives us the formula to transform the semi-infinite horizontal half-strip to the unit circle as,

$$\lambda(z) = \omega \circ \mu(z) = \frac{-\cosh z + i}{\cosh z + i} \tag{2.7}$$

But again, we need to be careful about our μ. We investigate the error by plotting the resultant map using MATLAB, see figure 2.6. A big error occurred during transformation $\mu = \cosh z$.
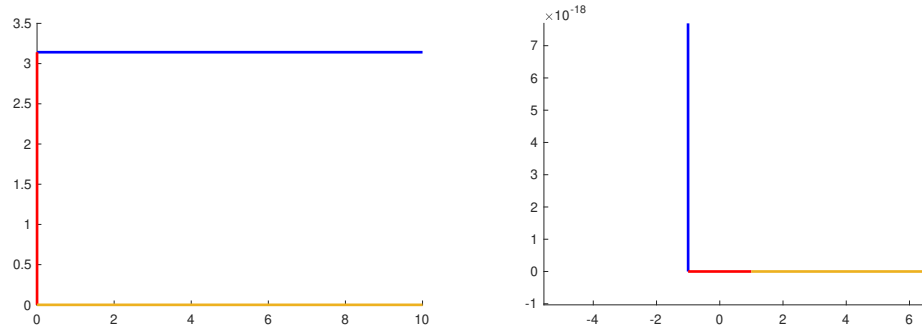
Figure 2.6. Visualization of the conformal map μ before treatment

To treat this map, we first rewrite the function $\mu = \cosh z$ in exponential form, then we find another trigonometric formula as,

$$\begin{aligned}
\cosh z &= \frac{e^z + e^{-z}}{2} = \frac{e^{x+iy} + e^{-(x+iy)}}{2} = \frac{e^x e^{iy} + e^{-x} e^{-iy}}{2} \\
&= \frac{e^x(\cos y + i \sin y) + e^{-x}(\cos y - i \sin y)}{2} \\
&= \frac{\cos y(e^x + e^{-x})}{2} + \frac{i \sin y(e^x - e^{-x})}{2} \\
&= \cos y \cosh x + i \sin y \sinh x.
\end{aligned}$$

8

Now, we substitute y values of the boundaries and define the maps separately. For the boundary on $y = \pi$, we get $\mu = -\cosh x$, and for the boundary on $y = 0$, we have $\mu = \cosh x$. It can be understood from figure 2.7, the map is more reliable after treatment.
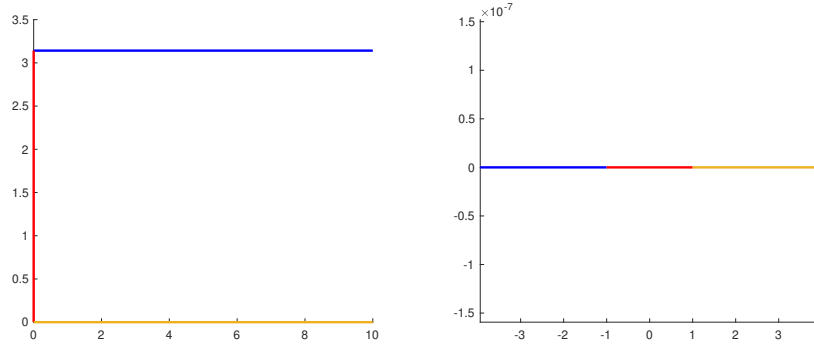
Figure 2.7. Visualization of the conformal map μ after treatment

Definition 2.3 *Inverse of the conformal map* (2.7) *can be found as,*

$$z = \cosh^{-1} \frac{i - i\mu}{\mu + 1}.$$

(2.8)

This time, we consider Γ_0 as

$$\Gamma_0 := \{z(t) = (r(t)\cos t + 2, r(t)\sin t + 3/2i),\ t \in [0, 2\pi]\}$$

where $r(t) = \sqrt{\cos^2 t + 0.25 \sin^2 t}$. We find the image by putting the equation of Γ_0 to the map (2.5). Visualization of the transformation is given in the figure 2.8.

2.2.3. Semi-infinite Vertical Half-Strip

Let the semi-infinite vertical strip be defined as $\Gamma_1 := \{(x, y) : -\pi/2 \leq x \leq \pi/2,\ 0 \leq y \leq \infty\}$. And the map $\eta(z) = \sin z$, it maps Γ_1 to the right half plane, for a detailed explanation see [16]. Also, by using the transformation (2.2), we can construct the map

9
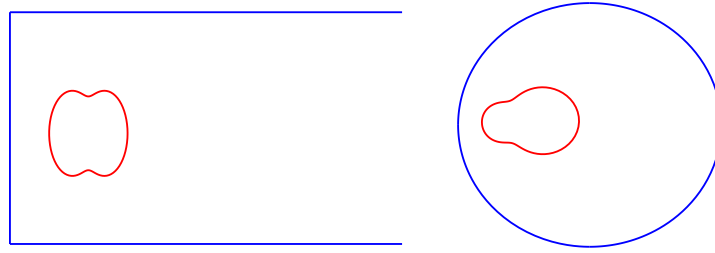
Figure 2.8. Visualization of the Transformation (2.7)

that sends the semi-infinite vertical strip to the unit circle, by composing η and ω

$$\theta(z) = \omega \circ \eta(z) = \frac{-\sin z + i}{\sin z + i} \tag{2.9}$$

This time, we need to check the map η, which maps the semi-infinite vertical half-strip to the upper half plane. The visualization of the transformation without treatment is given in the figure 2.9.
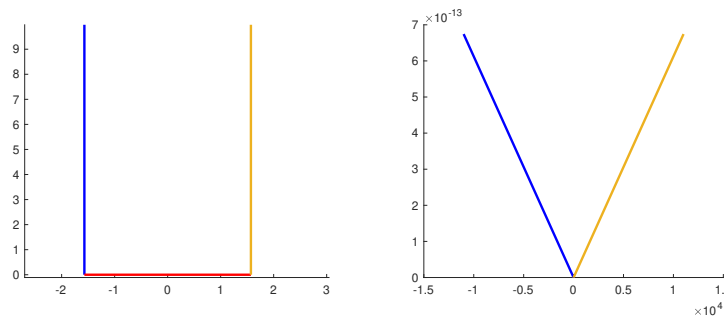
Figure 2.9. Visualization of the conformal map η before treatment

It can be understood from 2.9, a big error occurred during transformation. To avoid this error, we will transform the lines separately. To this end, we may use the same process with previous section to find $\eta(z)$. After some algebraic calculations, we find $\eta(z)$ as,

$$\eta(z) = \sin z = \sin x \cosh y + i \cos x \sinh y$$

Now, substituting x values of the boundaries and define the maps separately. For the boundary on $x = -\pi/2$, we have $\eta = -\cosh y$, and for the boundary on $x = \pi/2$, we get $\eta = \cosh y$. It can be understood from figure 2.10, the map is more reliable after treatment.
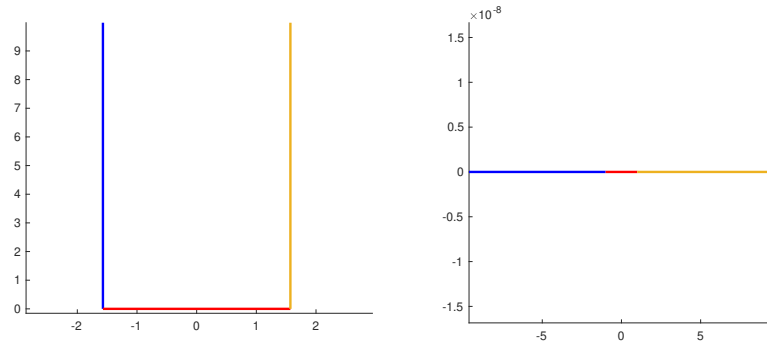
Figure 2.10. Visualization of the conformal map η after treatment

Definition 2.4 *Inverse of the map* (2.9) *can be found as,*

$$z = \arcsin \frac{1 - \theta i}{1 + \theta i} \tag{2.10}$$

In this domain, we consider Γ_0 as

$$\Gamma_0 := \{z(t) = (r(t) \cos t, r(t) \sin t + 2), \, t \in [0, 2\pi]\}$$

where $r(t) = \sqrt{\cos^2 t + 0.25 \sin^2 t}$. We find the image by putting the equation of Γ_0 to the map (2.9). Visualization of the transformation is given in the figure 2.9.

11
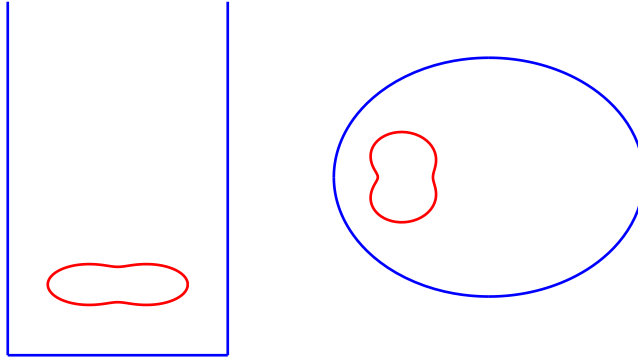
Figure 2.11. Visualization of the Transformation (2.9)

2.3. Image of the Boundary Conditions

In this section, reflections of Dirichlet and Neumann Type boundary conditions on unit circle will be explained. Some calculations that are made to find the images of boundary conditions are done by using MATLAB due to their computational cost.

2.3.1. Dirichlet Type Boundary Conditions

Theorem 2.2 (Olver, 2017) *If $U(\xi, \eta)$ is a harmonic function of ξ, η, and*

$$\omega = \xi + i\eta = \xi(x, y) + i\eta(x, y) = g(z)$$

is any analytic function, then the composition

$$u(x, y) = U(\xi(x, y), \eta(x, y)) \tag{2.11}$$

is a harmonic function of x, y.

The change of variables formula (2.11) from Theorem 2.2 will map the function $u(x, y)$ on D to function $U(\xi, \eta)$ on D', where u and U are both harmonic. Using formula (2.11)

the boundary values of $U = F$ and $U = G$ on the boundaries Γ_0' and Γ_1' correspond to those $u = f$ and $u = g$ on Γ_0 and Γ_1.

Theorem 2.3 *Let U be the solution of the problem in D' and $u = U \circ \omega$ be the solution in the original domain D with the Dirichlet boundary condition $u = f$ on ∂D. And the reflection of boundary condition can be written by using the formula,*

$$U = f \circ \omega^{-1} \text{ on } \partial D' \tag{2.12}$$

Example 2.1 (Dirichlet Condition Transformation for the Upper Half-Plane)
We have,
$$\omega(z) = \frac{-z + i}{z + i} \quad \Rightarrow \quad \frac{-x - iy + i}{x + iy + i}$$
that maps the upper half plane to the unit circle.
Then we may write, $u(x, y) = U(\xi(x, y), \eta(x, y))$ by separating real and imaginary parts;

$$\frac{-x + i(y - 1)}{x + i(y + 1)} = \frac{-x^2 - y^2 + 1}{x^2 + (y + 1)^2} + i\frac{2x}{x^2 + (y + 1)^2}$$

Then we have $\xi(x, y)$ and $\eta(x, y)$,

$$\xi(x, y) = \frac{-x^2 - y^2 + 1}{x^2 + (y + 1)^2}$$
$$\eta(x, y) = \frac{2x}{x^2 + (y + 1)^2}$$

where $U(\xi(x, y), \eta(x, y))$ satisfies Laplace Equation in upper half plane. Using equation (2.3), we can write,

$$U\left(\frac{-x^2 - y^2 + 1}{x^2 + (y + 1)^2}, \frac{2x}{x^2 + (y + 1)^2}\right) = \frac{i - i(x + iy)}{x + iy + 1}$$
$$= \frac{y + i(1 - x)}{x + 1 + iy} = \frac{2y}{(x + 1)^2 + y^2} + i\frac{1 - x^2 - y^2}{(x + 1)^2 + y^2}$$

Let $G(\theta) = U(\cos\theta, \sin\theta)$ be the value of u on Γ'_1. Then we put $U(\cos\theta, \sin\theta)$, to get;

$$\frac{2\sin\theta}{(\cos\theta+1)^2+\sin^2\theta} + i\frac{1-\cos^2\theta-\sin^2\theta}{(\cos\theta+1)^2+\sin^2\theta} \Rightarrow \frac{2\sin\theta}{(\cos\theta+1)^2+\sin^2\theta}$$

We take the expression of x since Γ_1 is the x axis. And after doing some simplification, the boundary condition on Γ'_1 becomes,

$$G(\theta) = g(\tan\frac{\theta}{2}) \tag{2.13}$$

It can be seen from the example, we are composing the boundary value f with the inverse of our map to find the image of Dirichlet condition. All other evaluations for the transformations of boundary conditions are made in this setting by using MATLAB.

2.3.2. Neumann Type Boundary Conditions

Theorem 2.4 *Let U be the solution of the problem in D' and $u = U \circ \omega$ be the solution in the original domain D with the Neumann boundary condition $\frac{\partial u}{\partial \nu} = f$ on Γ_0. Then the image of boundary condition can be written by using the formula,*

$$\frac{\partial U}{\partial \nu_{\Gamma'_0}}(\omega(\xi)) = \frac{1}{|\omega'(\xi)|}f(\xi) \tag{2.14}$$

Proof For a detailed construction and proof of the formula (2.14), see [15]. $\quad\square$

Example 2.2 *In the easiest case of Neumann type boundary values, we have $\frac{\partial u}{\partial \nu} = 0$, that is tangent vector and normal vector are orthogonal. Since conformal map preserves the angle between them, the image will be again $\frac{\partial U}{\partial \nu_{\Gamma'_0}}(\omega(\xi)) = 0$.*

CHAPTER 3

POTENTIAL THEORY

In this chapter, we give an explanation of the fundamental concepts and key theorems in potential theory. We establish the necessary foundations to construct representations of solutions in the next chapter by providing these fundamental definitions and theorems from [17].

Definition 3.1 *Fundamental solution of Laplace equation is given by*

$$\Phi(x,y) := \begin{cases} \frac{1}{2\pi} \ln \frac{1}{|x-y|} & m = 2 \\ \frac{1}{4\pi} \frac{1}{|x-y|} & m = 3. \end{cases}$$

Definition 3.2 *Given a function $\varphi \in C(\partial D)$,*

$$\text{Single-Layer Potential: } u(x) := \int_{\partial D} \varphi(y)\Phi(x,y)ds(y), \ x \in \mathbb{R}^2 \backslash \partial D, \qquad (3.1)$$

and

$$\text{Double-Layer Potential: } v(x) := \int_{\partial D} \varphi(y)\frac{\Phi(x,y)}{\partial \nu(y)}ds(y), \ x \in \mathbb{R}^2 \backslash \partial D, \qquad (3.2)$$

are defined.

One can see that kernel of the single-layer potential (3.1) is weakly singular and kernel of the double-layer potential (3.2) is continuous.

Theorem 3.1 (Kress, 2014) *Integral operators with continuous or weakly singular kernel are compact linear operators on $C(\partial D)$ if ∂D is of class C^1.*

Proof   Proof is given in detail in [17]   □

Theorem 3.1 implies that our operators are compact, we are going to use this information to prove our solutions depends continuously on the right hand side by using the following corollary from Riesz Theory.

Corollary 3.1 (Kress, 2014) *Let $A : X \to X$ be a compact linear operator on a normed space X. If the homogeneous equation*

$$\varphi - A\varphi = 0$$

only has the trivial solution $\varphi = 0$, then for each $f \in X$ the inhomogeneous equation

$$\varphi - A\varphi = f$$

has a unique solution $\varphi \in X$ and this solution depends continuously on the given boundary data.

Theorem 3.2 (Green's Formula) *Let D be a bounded domain of class C^1 and let $u \in C^2(\bar{D})$ be harmonic in D. Then*

$$u(x) = \int_{\partial D} \left\{ \frac{\partial u}{\partial \nu}(y)\Phi(x,y) - u(y)\frac{\partial \Phi(x,y)}{\partial \nu(y)} \right\} ds(y), \ x \in D. \tag{3.3}$$

Theorem 3.2 shows that any solution of Laplace Equation can be represented by using single- and double-layer potentials.

Theorem 3.3 (Kress, 2014) *For ∂D of class C^2, the double-layer potential v with continuous density φ can be continuously extended from D to $\bar{D}$ and from $\mathbb{R}^2 \backslash \bar{D}$ to $\mathbb{R}^2 \backslash D$ with limiting values,*

$$v_\pm(x) = \int_{\partial D} \varphi(y)\frac{\Phi(x,y)}{\partial \nu(y)}ds(y) \pm \frac{1}{2}\varphi(x), x \in \partial D, \tag{3.4}$$

where

$$v_\pm(x) := \lim_{h \to +0} v(x \pm h\nu(x)).$$

And for the single-layer potential with continuous density ψ we have

$$\frac{\partial u_\pm}{\partial \nu}(x) = \int_{\partial D} \psi(y)\frac{\Phi(x,y)}{\partial \nu(x)}ds(y) \mp \frac{1}{2}\psi(x), x \in \partial D, \tag{3.5}$$

where

$$\frac{\partial u_\pm}{\partial \nu}(x) := \lim_{h \to +0} u(x) \cdot \mathrm{grad} u(x \pm h\nu(x))$$

and where the integrals exist as improper integrals.

Theorem 3.4 (Kress, 2014) *The operators $I - K$ and $I - K'$, have trivial nullspaces*

$$N(I - K) = N(I - K') = \{0\}$$

The nullspaces of the operators $I + K$ and $I + K'$ have dimension one and

$$N(I + K) = span\{1\}, \quad N(I + K') = span\{\psi_0\}.$$

Also the equation $I + K'$ is solvable if and only if $\langle f, \psi_0 \rangle = 0$, where f is the given boundary data. And where K and K' stands for the integrals in (3.4) *and* (3.5)*, respectively.*

3.1. Applications on Boundary Value Problems

In this section, we will introduce two applications of potential theory on boundary value problems for the Laplace Equation.

3.1.1. Green's Function Technique

As mentioned earlier, the problems can be solved in the original domain using Green's Function Technique by constructing the Greens Function for the corresponding semi-infinite domains. In this subsection, we will solve a Laplace boundary value problem subject to Dirichlet boundary conditions using Green's Function Technique to sketch the solution steps and to show the disadvantages of the method.

Problem:

Let $D_1 \subset \mathbb{R}^2$ be the upper half plane with boundary Γ_1, $D_0 \subset \mathbb{R}^2$ be a simply connected bounded domain with boundary Γ_0 of class C^2 such that $\bar{D}_0 \subset D_1$, and $D = D_1 \setminus \bar{D}_0$,

$\partial D = \Gamma_0 \cup \Gamma_1$ where $\Gamma_0 \cap \Gamma_1 = \emptyset$.

Given a function $f \in C(\Gamma_1)$, find a bounded solution $u \in C^2(D)$ to the Laplace Equation

$$\Delta u = 0 \ \ \text{in} \ \ D$$

that satisfies Dirichlet boundary conditions,

$$u(x) = 0 \ \ \text{on} \ \ \Gamma_0, \ u(x) = f \ \ \text{on} \ \ \Gamma_1.$$

Solution: To solve the problem using Green's Function Technique, we first need to find the Green's Function for Laplace Equation on upper half-plane. To this end, we rewrite our problem as,

$$\Delta G(x, x_0) = \delta(x - x_0), \ x \in D,$$
$$G(x, 0, x_0) = 0, \ \ \text{on} \ \Gamma_1.$$

For any x_0^*, any point on lower half plane, we know that $\delta(x - x_0^*) = 0$. Where,

$$\vec{x_0} = (x_0, y_0) \ \text{is a positive source, and}$$
$$\vec{x_0^*} = (x_0, -y_0) \ \text{is a negative source.}$$

Then,

$$
\begin{aligned}
G(x, x_0) &= \frac{1}{2\pi} \left(\ln |x - \vec{x_0}| - \ln |x - \vec{x_0^*}| \right) \\
&= \frac{1}{4\pi} \ln \frac{(x - x_0)^2 - (y - y_0)^2}{(x - x_0)^2 + (y + y_0)^2}.
\end{aligned}
\tag{3.6}
$$

Notice that equation (3.6) satisfies the homogeneous boundary conditions at $y = 0$. Now we may find the derivative with respect to y_0.

$$\frac{\partial G}{\partial y_0}(x, x_0) = \frac{1}{4\pi} \left(\frac{-2(y - y_0)}{(x - x_0)^2 + (y - y_0)^2} - \frac{2(y + y_0)}{(x - x_0)^2 + (y + y_0)^2} \right)$$

Thus, for $y_0 = 0$, we have

$$\frac{\partial G}{\partial y_0}(x, x_0)\bigg|_{y_0=0} = \frac{y/\pi}{(x - x_0)^2 + y^2} \tag{3.7}$$

The second thing to do is to find the representation for the solution u by using Green's Function. To do that, we recall the Green's Formula (3.2) and by using it we write the representation of the solution to the problem as follows,

$$u(x) = \int_{\Gamma_0} \left\{ \frac{\partial u}{\partial \nu}(y)G(x, y) - u(y)\frac{\partial G(x, y)}{\partial \nu(y)} \right\} ds(y) + \int_{\Gamma_1} \left\{ \frac{\partial u}{\partial \nu}(y)G(x, y) - u(y)\frac{\partial G(x, y)}{\partial \nu(y)} \right\} ds(y) \tag{3.8}$$

Then we substitute our boundary conditions to the equation (3.8), to get

$$u(x) = \int_{\Gamma_0} \frac{\partial u}{\partial \nu}(y)G(x, y)ds(y) - \int_{\Gamma_1} f(y)\frac{\partial G(x, y)}{\partial \nu(y)}ds(y), \ x \in D \tag{3.9}$$

We have,

$$\int_{\Gamma_0} \frac{\partial u}{\partial \nu}(x_0)G(x, x_0)ds(x_0) = \int_{\Gamma_1} f(x_0)\frac{\partial G(x, x_0)}{\partial \nu(x_0)}ds(x_0), \ x \in \Gamma_0 \tag{3.10}$$

Then we substitute $G(x, x_0)$ and $\frac{\partial G(x,x_0)}{\partial \nu(x_0)}$ to get,

$$\frac{1}{4\pi} \int_{\Gamma_0} \frac{\partial u}{\partial \nu}(x_0) \ln \frac{(x - x_0)^2 - (y - y_0)^2}{(x - x_0)^2 + (y - y_0)^2} dx_0 = \frac{1}{\pi} \int_{\Gamma_1} f(x_0)\frac{y}{(x - x_0)^2 + y^2} dx_0 \tag{3.11}$$

Hence, our problem is reduced to a Fredholm Integral Equation of the First Kind. Fredholm integral equations of the first kind are considered ill-posed problems in the literature, and that implies this Fredholm Integral Equation of the First Kind could have no unique

solution, and even if the solution exists, it may not depend continuously on the right-hand side. One can solve this kind of equations by using regularization methods, but still, it is not advantageous and needs a significant amount of effort.

3.1.2. Boundary Integral Equation Method

We call equations (3.4) and Theorem (3.5) jump relations for double- and single-layer potentials respectively. In the light of those jump relations and Theorem3.4, we state following theorems.

Theorem 3.5 (Kress, 2014) *The double-layer potential*

$$u(x) = \int_{\partial D} \varphi(y) \frac{\partial \Phi(x, y)}{\partial \nu(y)} ds(y), x \in D, \tag{3.12}$$

with continuous density φ is a solution to the interior Dirichlet problem provided that φ is a solution to the integral equation

$$\varphi(x) - 2 \int_{\partial D} \varphi(y) \frac{\partial \Phi(x, y)}{\partial \nu(y)} ds(y) = -2f(x), x \in \partial D. \tag{3.13}$$

In the case of Dirichlet problem, we need the double-layer potential on the exterior of Γ_0 which leads us to an integral equation, $\varphi + K\varphi = 2f$ for a continuous density function φ. $N(I + K') = span\{\psi_0\}$, by the Fredholm Theory [17]. But the equation is solvable if and only if $\langle f, \psi_0 \rangle = 0$. However, we cannot ensure that this condition is satisfied for arbitrary boundary data f. Therefore, the modified double-layer potential is introduced.

Theorem 3.6 (Kress, 2014) *The modified double-layer potential*

$$u(x) = \int_{\partial D} \varphi(y) \left(\frac{\partial \Phi(x, y)}{\partial \nu(y)} + \frac{1}{|x|^{m-2}} \right) ds(y), x \in \mathbb{R}^m \setminus \bar{D}, \tag{3.14}$$

with continuous density φ is a solution to the exterior Dirichlet problem provided that φ

is a solution of the integral equation

$$\varphi(x) + 2 \int_{\partial D} \varphi \left(\frac{\partial \Phi(x,y)}{\partial \nu(y)} + \frac{1}{|x|^{m-2}} \right) ds(y) = 2f(x), x \in \partial D. \qquad (3.15)$$

The modification on the Theorem 3.6 is true for $m > 2$. In the case of two dimensions, we need another modification, which will be introduced in Chapter 4.

Theorem 3.7 (Kress, 2014) *The single-layer potential*

$$u(x) := \int_{\partial D} \varphi(y) \Phi(x,y) ds(y), \ x \in \mathbb{R}^m \backslash D, \qquad (3.16)$$

with continuous density φ is a solution to the exterior Neumann problem provided that ψ is a solution of the integral equation,

$$\varphi(x) - 2 \int_{\partial D} \varphi(y) \frac{\partial \Phi(x,y)}{\partial \nu(x)} ds(y) = -2f(x), x \in \partial D. \qquad (3.17)$$

CHAPTER 4

BOUNDARY INTEGRAL EQUATIONS

In this chapter, with the help of the theorems stated in Chapter 3, we introduce representations to the solutions of boundary value problems. Using these representations, we construct corresponding systems of boundary integral equations of the second kind. It should be noted that the problems (1.2), (1.3) are equivalent to the systems of boundary integral equations that are constructed in this chapter. Finally, the chapter ends with the proof of the existence of unique solutions to the systems.

We seek to represent the solutions to both problems as a linear combination of double- and single-layer potentials. For this purpose, we introduce the integral operators $K, K', S : C(\partial D) \to C(\partial D)$ by,

$$(K\varphi)(x) = \int_{\partial D} \frac{\partial \Phi(x,y)}{\partial \nu(y)} \varphi(y) ds(y), \ x \in \partial D \tag{4.1}$$

$$(S\varphi)(x) = \int_{\partial D} \Phi(x,y)\varphi(y) ds(y), \ x \in \partial D \tag{4.2}$$

$$(K'\psi)(x) = \int_{\partial D} \frac{\partial \Phi(x,y)}{\partial \nu(x)} \psi(y) ds(y), \ x \in \partial D. \tag{4.3}$$

4.1. Dirichlet Problem

Modified double layer potential is introduced due to Theorem 3.4, but as mentioned in Chapter 3 it does not work for two dimensional case. This problem is solved by using a modification in [9]. But in this study, we introduce a different modification which is adding the single-layer potential to the boundary Γ'_0 and we represent our solution to the problem (1.1),(1.2) as,

$$u(x) = \int_{\Gamma'_0} \varphi(y) \left\{ \frac{\partial \Phi(x,y)}{\partial \nu(y)} + \Phi(x,y) \right\} ds(y) + \int_{\Gamma'_1} \psi(y) \frac{\partial \Phi(x,y)}{\partial \nu(y)} ds(y), x \in D. \tag{4.4}$$

Using the representation (4.4) and the jump relations of the double-layer potential (3.4), we can write the corresponding system of boundary integral equations as,

$$\frac{1}{2}\varphi(x) + \int_{\Gamma_0'} \varphi(y) \left(\frac{\partial \Phi(x,y)}{\partial \nu(y)} + \Phi(x,y) \right) ds(y) + \int_{\Gamma_1'} \psi(y) \frac{\partial \Phi(x,y)}{\partial \nu(y)} ds(y) = f(x), x \in \Gamma_0'$$

$$-\frac{1}{2}\psi(x) + \int_{\Gamma_0'} \varphi(y) \left(\frac{\partial \Phi(x,y)}{\partial \nu(y)} + \Phi(x,y) \right) ds(y) + \int_{\Gamma_1'} \psi(y) \frac{\partial \Phi(x,y)}{\partial \nu(y)} ds(y) = g(x), x \in \Gamma_1'$$

(4.5)

Theorem 4.1 *The system of integral equations for the Dirichlet problem* (4.5) *has a unique solution which depends continuously on the given boundary data.*

Proof   For the proof, we use Riesz theory [17] and show that the homogeneous system has only the trivial solution $\varphi = \psi = 0$.

Since our partial differential equation has a unique solution, it implies that $u \equiv 0$ in D'. And hence

$$\left. \frac{\partial u}{\partial \nu} \right|_{\Gamma_0'} = \left. \frac{\partial u}{\partial \nu} \right|_{\Gamma_1'} = 0$$

Let D_0' be the domain bounded by the curve Γ_0', then u_0 can be represented as

$$u_0(x) = \int_{\Gamma_0'} \varphi(y) \left\{ \frac{\partial \Phi(x,y)}{\partial \nu(y)} + \Phi(x,y) \right\} ds(y) + \int_{\Gamma_1'} \psi(y) \frac{\partial \Phi(x,y)}{\partial \nu(y)} ds(y), x \in D_0'$$

which solves $\Delta u_0 = 0$ in D_0'.

And let u_1 be the solution on $\mathbb{R}^2 \setminus \overline{D_0' \cup D'}$, we have

$$u_1(x) = \int_{\Gamma_0'} \varphi(y) \left\{ \frac{\partial \Phi(x,y)}{\partial \nu(y)} + \Phi(x,y) \right\} ds(y) + \int_{\Gamma_1'} \psi(y) \frac{\partial \Phi(x,y)}{\partial \nu(y)} ds(y), x \in \mathbb{R}^2 \setminus \overline{D_0' \cup D'}$$

solves $\Delta u_1 = 0$ in $\mathbb{R}^2 \setminus \overline{D_0' \cup D'}$.

From the jump relations of double-layer potential, we get

$$u_0(x) = -\varphi(x), \ \ x \in \Gamma_0'$$

23

And using the jump relations of single-layer potential, we also get

$$\frac{\partial u_0}{\partial \nu}(x) = \varphi(x), \ \ x \in \Gamma'_0$$

By using Greens First Theorem [17], we can write

$$\int_{D_0} (u_0 \Delta u_0 + \operatorname{grad} u_0 \cdot \operatorname{grad} u_0) dx = \int_{\Gamma_0} u_0 \frac{\partial u_0}{\partial \nu} ds \Rightarrow \int_{D_0} |\operatorname{grad} u_0|^2 dx = - \int_{\Gamma_0} \varphi^2 ds$$

which implies $\varphi = 0$. Ans since $\varphi = 0$, the second equation becomes,

$$-\frac{1}{2}\psi(x) + \int_{\Gamma'_1} \psi(y) \frac{\partial \Phi(x, y)}{\partial \nu(y)} ds(y) = 0, x \in \Gamma'_1$$

which can be written in the operator form as $(-I/2 + K)\psi = 0$, using Theorem 3.4 we conclude that $\psi = 0$. $\qquad\square$

4.2. Mixed Problem

In the case of Mixed boundary conditions, such modification (4.4) is not needed. We represent the solution to the problem (1.1),(1.3) as,

$$u(x) = \int_{\Gamma'_0} \varphi(y) \Phi(x, y) ds(y) + \int_{\Gamma'_1} \psi(y) \frac{\partial \Phi(x, y)}{\partial \nu(y)} ds(y) , x \in D' \qquad (4.6)$$

Using representation (4.6) and the jump relations for double-layer (3.4) and single-layer (3.5) potentials, we can write the corresponding system of boundary integral equations as,

$$-\frac{1}{2}\varphi(x) + \int_{\Gamma'_0} \varphi(y) \frac{\partial \Phi(x, y)}{\partial \nu(x)} ds(y) + \frac{\partial}{\partial \nu(x)} \int_{\Gamma'_1} \psi(y) \frac{\partial \Phi(x, y)}{\partial \nu(y)} ds(y) = f, \quad x \in \Gamma'_0$$

$$-\frac{1}{2}\psi(x) + \int_{\Gamma'_0} \varphi(y) \Phi(x, y) ds(y) + \int_{\Gamma'_1} \psi(y) \frac{\partial \Phi(x, y)}{\partial \nu(y)} ds(y) = g, \quad x \in \Gamma'_1$$

$$(4.7)$$

24

Theorem 4.2 *The system of integral equations for the Mixed problem* (4.7) *has a unique solution which depends continuously on the given boundary data.*

Proof   Again, by using Riesz Theory, we need to show $\varphi = \psi = 0$.

Let u_0 be the solution inside Γ_0', it solves

$$\Delta u_0 = 0 \text{ in } D_0' \tag{4.8}$$

$$\frac{\partial u_0}{\partial \nu} = 0 \text{ on } \Gamma_0' \tag{4.9}$$

problem (4.8)-(4.9) implies that $u_0 = c$ in D_0. And we can write the jump relations as,

$$\frac{\partial u}{\partial \nu}(x) = -\frac{1}{2}\varphi(x) + \int_{\Gamma_0'} \varphi(y)\frac{\partial \Phi(x,y)}{\partial \nu(x)} ds(y) + \frac{\partial}{\partial \nu(x)} \int_{\Gamma_1'} \psi(y)\frac{\partial \Phi(x,y)}{\partial \nu(y)} ds(y), \ x \in \Gamma_0'$$

$$\frac{\partial u_0}{\partial \nu}(x) = \frac{1}{2}\varphi(x) + \int_{\Gamma_0'} \varphi(y)\frac{\partial \Phi(x,y)}{\partial \nu(x)} ds(y) + \frac{\partial}{\partial \nu(x)} \int_{\Gamma_1'} \psi(y)\frac{\partial \Phi(x,y)}{\partial \nu(y)} ds(y), \ x \in \Gamma_0'$$

And the difference will be

$$\frac{\partial u}{\partial \nu}(x) - \frac{\partial u_0}{\partial \nu}(x) = -\varphi(x), \ x \in \Gamma_0'.$$

Since

$$\frac{\partial u}{\partial \nu}(x) = \frac{\partial u_0}{\partial \nu}(x) = 0, \ x \in \Gamma_0'$$

holds, we conclude that $\varphi = 0$. Therefore, the second equation of the system becomes,

$$-\frac{1}{2}\psi(x) + \int_{\Gamma_1'} \psi(y)\frac{\partial \Phi(x,y)}{\partial \nu(y)} ds(y) = 0, x \in \Gamma_1'$$

From the Theorem 3.4 we know that

$$N(-I + K) = \{0\}$$

which implies that $\psi = 0$.   □

CHAPTER 5

NUMERICAL METHOD

In this chapter, we provide general information about quadrature rules and introduce a formula for improper integrals. Besides we explain the Nyström Method for the numerical solution of Integral Equations of the second kind. Then we parameterize our double- and single-layer potential operators and introduce our numerical integration operators.

5.1. Quadrature Rules

An integral

$$Q(f) = \int_D f(x)dx, \tag{5.1}$$

with $f \in C(D)$, can be approximated by the weighted sum

$$Q_n(f) = \sum_{k=1}^{n} \alpha_k f(x_k), \tag{5.2}$$

where α_k are known weights and x_k are the quadrature points.

Theorem 5.1 (Steklov) *Assume $Q_n(1) \to Q(1)$ as $n \to \infty$ and the quadrature weights are positive. Then the quadrature formulas (Q_n) converge if and only if $Q_n(1) \to Q(1)$ as $n \to \infty$, for all f in some dense subset $U \subset C(D)$.*

Proof   Proof is given in [17]. $\qquad\qquad\qquad\qquad\qquad\qquad\qquad\qquad\qquad\square$

For the improper integrals, the classical quadrature rules are not convenient. Due to this reason, we introduce another quadrature formula which is extremely accurate for improper integrals whose integrand is 2π periodic functions with logarithmic singularity.

Let φ be a 2π periodic continuous function,

$$(A\varphi)(t) := \int_0^{2\pi} \frac{1}{2\pi} \ln |4\sin^2 \frac{t-\tau}{2}| k(t,\tau)\varphi(\tau)d\tau, \ \ t \in [0, 2\pi]$$

and it can be approximated by the formula,

$$(A_n\varphi)(t) := \sum_{j=0}^{2n-1} R_j^{(n)}(t)k(t,t_j)\varphi(t_j) \tag{5.3}$$

which is constructed by substituting trigonometric interpolation polynomial instead of φ and using Lagrange basis with the equidistantly distributed points $t_j = \frac{j\pi}{n}$ and the weights,

$$R_j^{(n)}(t) = -\frac{1}{n}\left[\sum_{m=1}^{n-1}\frac{1}{m}\cos(m(t-t_j)) + \frac{1}{2n}\cos(n(t-t_j))\right], \; j = 0,..,2n-1. \tag{5.4}$$

The quadrature rule (5.3) converges uniformly for all trigonometric polynomials, for the proof see [17].

5.2. Error Estimates

We know that Trapezoidal rule for trigonometric functions is exponentially convergent due to its asymptotic error formula, see ([18], p.212) for a detailed explanation. Therefore, we use the following error estimate.

Theorem 5.2 *Let $g : \mathbb{R} \to \mathbb{R}$ be analytic and 2π periodic. Then the error,*

$$R_T(g) := \int_a^b g(x)dx - \frac{1}{2n}\sum_{i=0}^{2n-1} g\left(\frac{i\pi}{n}\right), \tag{5.5}$$

for composite trapezoidal rule can be estimated by,

$$|R_T(g)| \leq Ce^{-2ns}, \tag{5.6}$$

where C and s are positive constants depending on g.

Theorem 5.2 shows that Trapezoidal Rule converges exponentially fast for periodic analytic functions. In this sense, it will be wise to use Nyström Method based on trapezoidal

rule to approximate the continuous kernels.

5.3. Nyström Method

Let φ_n be a solution of

$$\varphi_n(x) - \sum_{k=1}^{n} \alpha_k K(x, x_k)\varphi_n(x_k) = f(x), \ x \in D.$$

Then the values $\varphi_j^{(n)} = \varphi_n(x_j)$, $j = 1, ..., n$ at the quadrature points satisfy the linear system

$$\varphi_j^{(n)} - \sum_{k=1}^{n} \alpha_k K(x_j, x_k)\varphi_k^{(n)} = f(x_j), \ j = 1, ..., n \tag{5.7}$$

or alternatively, in operator form,

$$\varphi_n - A_n\varphi_n = f.$$

Conversely, we can find φ_n by,

$$\varphi_n(x) := f(x) + \sum_{k=1}^{n} \alpha_k K(x_j, x_k)\varphi_k^{(n)} \tag{5.8}$$

Theorem 5.3 (Kress, 2012) *If the quadrature formulas of* (5.7) *are convergent. Then the sequence A_n is collectively compact and pointwise convergent, i.e. $A_n\varphi_n \to A\varphi$, $n \to \infty$, for all $\varphi \in C(D)$.*

As can be seen from Theorem 5.3 the matrix and the right hand side of the linear system (5.7) are obtained by evaluating the kernel and the given function at the quadrature nodes. Therefore, by using a more accurate quadrature rule, we can significantly improve the approximations without putting any additional computational work into it. Additionally, condition number of the matrix (5.8) gives us an idea about the stability of the method.

5.4. Parameterized Operators

We use a parametric representation with,

$$\Gamma'_0 := \{z(t) = (z_1(t), z_2(t)) : t \in [0, 2\pi]\}$$
$$\Gamma'_1 := \{\xi(t) = (\xi_1(t), \xi_2(t)) : t \in [0, 2\pi]\}$$

And we can define our parameterized operators for Dirichlet problem as,

$$(K_{00}\varphi)(t) = \int_0^{2\pi} \frac{\partial \Phi(z(t), z(\tau))}{\partial \nu(z(\tau))} |z'(\tau)| \varphi(\tau) d\tau, \ t \in [0, 2\pi] \tag{5.9}$$

$$(S_{00}\varphi)(t) = \int_0^{2\pi} \Phi(z(t), z(\tau)) |z'(\tau)| \varphi(\tau) d\tau, \ t \in [0, 2\pi] \tag{5.10}$$

$$(K_{01}\psi)(t) = \int_0^{2\pi} \frac{\partial \Phi(z(t), \xi(\tau))}{\partial \nu(\xi(\tau))} |\xi'(\tau)| \psi(\tau) d\tau, \ t \in [0, 2\pi] \tag{5.11}$$

$$(K_{10}\varphi)(t) = \int_0^{2\pi} \frac{\partial \Phi(\xi(t), z(\tau))}{\partial \nu(z(\tau))} |z'(\tau)| \varphi(\tau) d\tau, \ t \in [0, 2\pi] \tag{5.12}$$

$$(S_{10}\varphi)(t) = \int_0^{2\pi} \Phi(\xi(t), z(\tau)) |z'(\tau)| \varphi(\tau) d\tau, \ t \in [0, 2\pi] \tag{5.13}$$

$$(K_{11}\psi)(t) = \int_0^{2\pi} \frac{\partial \Phi(\xi(t), \xi(\tau))}{\partial \nu(\xi(\tau))} |\xi'(\tau)| \psi(\tau) d\tau, \ t \in [0, 2\pi] \tag{5.14}$$

and for the Mixed problem we define our parameterized operators as,

$$(K'_{00}\varphi)(t) = \int_0^{2\pi} \frac{\partial \Phi(z(t), z(\tau))}{\partial \nu(z(t))} |z'(\tau)| \varphi(\tau) d\tau, \ t \in [0, 2\pi] \tag{5.15}$$

$$(S_{10}\varphi)(t) = \int_0^{2\pi} \Phi(z(t), \xi(\tau)) |\xi'(\tau)| \varphi(\tau) d\tau, \ t \in [0, 2\pi] \tag{5.16}$$

$$(K_{11}\psi)(t) = \int_0^{2\pi} \frac{\partial \Phi(\xi(t), \xi(\tau))}{\partial \nu(\xi(\tau))} |\xi'(\tau)| \psi(\tau) d\tau, \ t \in [0, 2\pi] \tag{5.17}$$

$$(T_{01}\psi)(t) = \frac{\partial}{\partial \nu(z(t))} \int_0^{2\pi} \frac{\partial \Phi(z(t), \xi(\tau))}{\partial \nu(\xi(\tau))} |\xi'(\tau)| \psi(\tau) d\tau, \ t \in [0, 2\pi] \tag{5.18}$$

where $|z'(\tau)|, |\xi'(\tau)| > 0$.

The Double-Layer Potential operator is continuous with the limiting values,

$$\frac{\partial \Phi(z(t), z(\tau))}{\partial \nu(z(\tau))} = \begin{cases} \frac{1}{\pi} \frac{[z'(\tau)]^{\perp} \cdot \{z(t) - z(\tau)\}}{|z(t) - z(\tau)|^2} & t \neq \tau \\ \frac{1}{2\pi} \frac{[z'(t)]^{\perp} \cdot z''(t)}{|z'(t)|^2} & t = \tau. \end{cases}$$

The adjoint of Double-Layer Potential operator is continuous with the limiting values,

$$\frac{\partial \Phi(z(t), z(\tau))}{\partial \nu(z(t))} = \begin{cases} -\frac{1}{\pi} \frac{[z'(t)]^{\perp}}{|z'(t)|} \cdot \frac{\{z(t) - z(\tau)\}}{|z(t) - z(\tau)|^2} |z'(\tau)| & t \neq \tau \\ \frac{1}{2\pi} \frac{[z'(t)]^{\perp} \cdot z''(t)}{|z'(t)|^2} & t = \tau. \end{cases}$$

The Single-Layer Potential operator has a weakly singular kernel, to deal with that singularity we apply a method which is used in [17]. We split off the singularity in the kernel of integral operator. And the kernel can be represented as a difference of a singular part and a continuous part,

$$\int_0^{2\pi} \frac{1}{2\pi} \ln \frac{|4 \sin^2 \frac{t-\tau}{2}|}{|z(t) - z(\tau)|^2} \varphi(\tau) d\tau - \int_0^{2\pi} \frac{1}{2\pi} \ln |4 \sin^2 \frac{t-\tau}{2}| \varphi(\tau) d\tau$$

First integrand, denoted by $\widetilde{S}$, is smooth with the diagonal values,

$$(\widetilde{S}\psi)(t) = \begin{cases} \frac{1}{2\pi} \ln \frac{|4 \sin^2 \frac{t-\tau}{2}|}{|z(t) - z(\tau)|^2} & t \neq \tau \\ -\frac{1}{2\pi} \ln |z'(t)^2| & t = \tau. \end{cases}$$

Since the second integral is improper, we use the quadrature formula 5.3,

$$\int_0^{2\pi} \frac{1}{2\pi} \ln |4 \sin^2 \frac{t-\tau}{2}| \varphi(\tau) d\tau \approx \sum_{j=0}^{2n-1} R_j^{(n)}(t) \varphi(t_j)$$

where,

$$R_j^{(n)}(t) = -\frac{1}{n} \sum_{m=1}^{n-1} \frac{1}{m} \cos(m(t - t_j)) + \frac{1}{2n} \cos(n(t - t_j)), \ j = 0, .., 2n - 1.$$

30

Since this splitting off the singularity method is based on exact integration, it is more accurate than other methods which take weakly singular integrals, for more applications see [19],[20].

Now we can introduce our numerical integration operators for Dirichlet problem, using Nyström's Method [17], for (5.9), (5.10), (5.14) as

$$(K_n\varphi)(t) := \sum_{k=1}^{n} \alpha_k K(t, \tau_k^{(n)})\varphi(\tau_k^{(n)}), \ t \in [0, 2\pi] \qquad (5.19)$$

$$(S_n\varphi)(t) := \sum_{k=1}^{n} \alpha_k K(t, \tau_k^{(n)})\varphi(\tau_k^{(n)}) - R^{(n)}(t)\varphi(t), \ t \in [0, 2\pi] \qquad (5.20)$$

$$(K_n\psi)(t) := \sum_{k=1}^{n} \alpha_k T(t, \tau_k^{(n)})\psi(\tau_k^{(n)}), \ t \in [0, 2\pi]. \qquad (5.21)$$

And we introduce our numerical integration operators for Mixed problem, using Nyström's Method [17], the approximations for (5.15),(5.16),(5.17),(5.18) are given respectively

$$(K_n\varphi)(t) := \sum_{k=1}^{n} \alpha_k K(t, \tau_k^{(n)})\varphi(\tau_k^{(n)}), \ t \in [0, 2\pi] \qquad (5.22)$$

$$(S_n\varphi)(t) := \sum_{k=1}^{n} \alpha_k K(t, \tau_k^{(n)})\varphi(\tau_k^{(n)}) - R^{(n)}(t)\varphi(t), \ t \in [0, 2\pi] \qquad (5.23)$$

$$(K_n\psi)(t) := \sum_{k=1}^{n} \alpha_k K(t, \tau_k^{(n)})\psi(\tau_k^{(n)}), \ t \in [0, 2\pi] \qquad (5.24)$$

$$(T_n\psi)(t) := \sum_{k=1}^{n} \alpha_k T(t, \tau_k^{(n)})\psi(\tau_k^{(n)}), \ t \in [0, 2\pi]. \qquad (5.25)$$

Then we have a system of linear equations for each problem which can also be represented as,

$$\begin{bmatrix} (\frac{I}{2} + K_{00}) & K_{01} \\ -K_{10} & (\frac{I}{2} - K_{11}) \end{bmatrix} \begin{bmatrix} \varphi \\ -\psi \end{bmatrix} = \begin{bmatrix} f \\ -g \end{bmatrix} \qquad (5.26)$$

or alternatively $(I + A)x = b$, and

$$\begin{bmatrix} (-\frac{I}{2} + K'_{00}) & T_{01} \\ S_{10} & (-\frac{I}{2} + K_{11}) \end{bmatrix} \begin{bmatrix} \varphi \\ \psi \end{bmatrix} = \begin{bmatrix} f \\ g \end{bmatrix} \qquad (5.27)$$

or alternatively $(-I + A)x = b$, for the Dirichlet and Mixed problems respectively. The systems (5.26), (5.27) can be solved by using Gaussian Elimination [21], [22].

CHAPTER 6

NUMERICAL EXAMPLES

In this chapter, both cases of the problem are considered to test the accuracy of the proposed method. To demonstrate that, some numerical examples with and without exact solutions are provided. We consider Γ_0 as given in the sections 2.1, 2.2.1, 2.2.2, and 2.2.3, respectively. The visualizations of conformal maps are given in Chapter 2.

6.1. Test Cases

To test the proposed method we solve a boundary value problem on the unit circle, where $x^* = (1.1, 1.1)$ and $x = (-0.5, 0.5)$.

Example 6.1 *We solve the Dirichlet Problem with the following boundary conditions*

$$\Delta u = 0 \ in \ D' \tag{6.1}$$

$$u(x) = -\frac{1}{2\pi} \ln |x - x^*| \ on \ \Gamma'_0 \tag{6.2}$$

$$u(x) = -\frac{1}{2\pi} \ln |x - x^*| \ on \ \Gamma'_1. \tag{6.3}$$

Since our boundary conditions are the fundamental solution of Laplace equation, the exact solution will be,

$$u(x) = -\frac{1}{2\pi} \ln |x - x^*|$$

Example 6.2 *We solve the Mixed Problem with the following boundary conditions*

$$\Delta u = 0 \ in \ D' \tag{6.4}$$

$$\frac{\partial u}{\partial \nu}(x) = -\frac{1}{2\pi} \frac{(x - x^*)}{|x - x^*|^2} \cdot \nu(x) \ on \ \Gamma'_0 \tag{6.5}$$

$$u(x) = -\frac{1}{2\pi} \ln |x - x^*| \ on \ \Gamma'_1 \tag{6.6}$$

Table 6.1. Numerical result for the point $(-0.5, 0.5)$

n	$\tilde{u}$	Error
8	-0.08579349	5.1957×10^{-4}
16	-0.08527595	2.0314×10^{-6}
32	-0.08527391	3.1014×10^{-11}
64	-0.08527391	2.7755×10^{-17}

Since our boundary conditions are the fundamental solution of Laplace equation and its normal derivative, the exact solution is again the fundamental solution of Laplace Equation. Note that solution is not evaluated at the blue regions.

Table 6.2. Numerical result for the point $(-0.5, 0.5)$

n	$\tilde{u}$	Error
8	-0.08579409	5.2018×10^{-4}
16	-0.08527594	2.0303×10^{-6}
32	-0.08527391	3.1014×10^{-11}
64	-0.08527391	1.3877×10^{-17}

In Tables 6.1 and 6.2, we have achieved the exponential convergence as expected, see section 5.2.
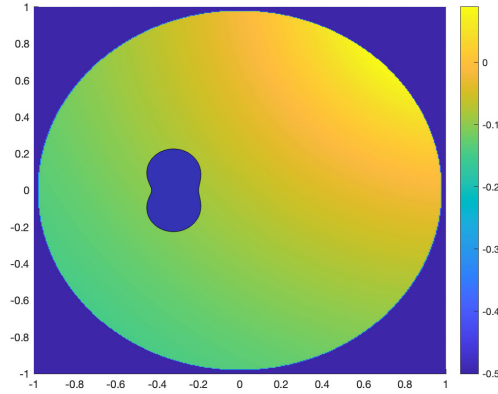
Figure 6.1. Solution in Domain

Since we tested the convergence of the proposed method, we can solve a problem which we don't know the exact solution.

6.2. Numerical Examples for the Problems Defined on Upper-Half Plane

In this section, we illustrate our method's approximation results for Dirichlet and Mixed Problems on Upper-Half Plane with a peanut-shaped hole, see Figure 2.2. The numerical solution with 256 quadrature points is considered as our exact solution to evaluate error and order of convergence.

Example 6.3 (Dirichlet Problem) *We try to get the solution to the problem that involves finding a function that satisfies the following boundary conditions and the Laplace Equation within the original domain,*

$$\Delta u = 0 \ \ in \ \ D$$
$$u(x) = 0 \ \ on \ \ \Gamma_0$$
$$u(x) = e^{-x^2} \ \ on \ \ \Gamma_1$$

Using the map (2.2)*, we transform the problem from unbounded domain to a bounded*

domain, we can write our transformed problem as

$$\Delta U = 0 \ \ in \ \ D'$$

$$U(\theta) = 0 \ \ on \ \ \Gamma_0'$$

$$U(\theta) = e^{-\tan^2(\frac{\theta}{2})} \ \ on \ \ \Gamma_1'$$

Table 6.3.   Results are evaluated at the point $(-0.5, 0.5)$ which corresponds to the point $(2, 1)$ of the original domain

n	$\tilde{u}$	*Error*	*Order of Convergence*
8	0.21148507	7.9841×10^{-4}	-
16	0.21068958	2.9189×10^{-6}	8.0956
32	0.21068666	1.2507×10^{-10}	14.5104
64	0.21068666	1.3878×10^{-16}	18.7815

Example 6.4 (Dirichlet Problem) *We try to get the solution to the problem that involves finding a function that satisfies the following boundary conditions and the Laplace Equation within the original domain,*

$$\Delta u = 0 \ \ in \ \ D$$

$$u(x) = 0 \ \ \ on \ \ \Gamma_0$$

$$u(x) = \frac{1}{x^2 + 1} \ \ on \ \ \Gamma_1$$

Using the map (2.2), we transform the problem from unbounded domain to a bounded domain, we can write our transformed problem as

$$\Delta U = 0 \ \ in \ \ D'$$

$$U(\theta) = 0 \ \ on \ \ \Gamma_0'$$

$$U(\theta) = \frac{1}{\tan^2(\frac{\theta}{2}) + 1} \ \ on \ \ \Gamma_1'$$

Table 6.4. Results are evaluated at the point $(-0.5, 0.5)$ which corresponds to the point $(2, 1)$ of the original domain

n	$\tilde{u}$	Error	Order of Convergence
8	0.3529	0.0026	-
16	0.3503	1.0410×10^{-5}	7.9832
32	0.3503	2.5283×10^{-10}	15.3295
64	0.3503	1.1102×10^{-16}	21.1189

Example 6.5 (Mixed Problem) *We try to get the solution to the problem that involves finding a function that satisfies the following boundary conditions and the Laplace Equation within the original domain,*

$$\Delta u = 0 \ \ in \ \ D$$
$$\frac{\partial u}{\partial \nu}(x) = 0 \ \ on \ \ \Gamma_0$$
$$u(x) = e^{-x^2} \ \ on \ \ \Gamma_1$$

Using the map (2.2), we transform the problem from unbounded domain to a bounded domain, we can write our transformed problem as

$$\Delta U = 0 \ \ in \ \ D'$$
$$\frac{\partial U}{\partial \nu}(\theta) = 0 \ \ on \ \ \Gamma'_0$$
$$U(\theta) = e^{-\tan^2(\frac{\theta}{2})} \ \ on \ \ \Gamma'_1$$

Table 6.5. Results are evaluated at the point $(-0.5, 0.5)$ which corresponds to the point $(2, 1)$ of the original domain

n	$\tilde{u}$	Error	Order of Convergence
8	0.35305438	3.7928×10^{-4}	-
16	0.35268197	6.8716×10^{-6}	5.7864
32	0.35267510	1.8419×10^{-9}	11.8652
64	0.35267510	5.5511×10^{-17}	24.5839

Example 6.6 (Mixed Problem) *We try to get the solution to the problem that involves finding a function that satisfies the following boundary conditions and the Laplace Equation within the original domain,*

$$\Delta u = 0 \ \ in \ \ D$$

$$u(x) = 0 \ \ \ on \ \ \Gamma_0$$

$$u(x) = \frac{1}{x^2 + 1} \ \ on \ \ \Gamma_1$$

Using the map (2.2), we transform the problem from unbounded domain to a bounded domain, we can write our transformed problem as

$$\Delta U = 0 \ \ in \ \ D'$$

$$\frac{\partial U}{\partial \nu}(\theta) = 0 \ \ on \ \ \Gamma_0'$$

$$U(\theta) = \frac{1}{\tan^2(\frac{\theta}{2}) + 1} \ \ on \ \ \Gamma_1'$$

Table 6.6. Results are evaluated at the point $(-0.5, 0.5)$ which corresponds to the point $(2, 1)$ of the original domain

n	$\tilde{u}$	Error	Order of Convergence	Condition Number
8	0.50496794	1.8339×10^{-3}	-	10.989
16	0.50496794	1.4373×10^{-5}	5.7864	10.943
32	0.50313396	2.2441×10^{-9}	11.8652	10.943
64	0.50313396	2.2204×10^{-16}	24.5839	10.943

Example 6.7 *Another interesting investigation of this method might be finding the infinity norm of the error at a specified region, we can take a region P from D and map the points to the transformed domain D'. For the test problems (6.1)-(6.3) and (6.4)-(6.6), the visualization of the transformation of a region is given in Figure 6.2. The problems are solved by taking same boundary conditions as in examples 6.1 and 6.2. And the relative error results are listed in Table 6.7.*
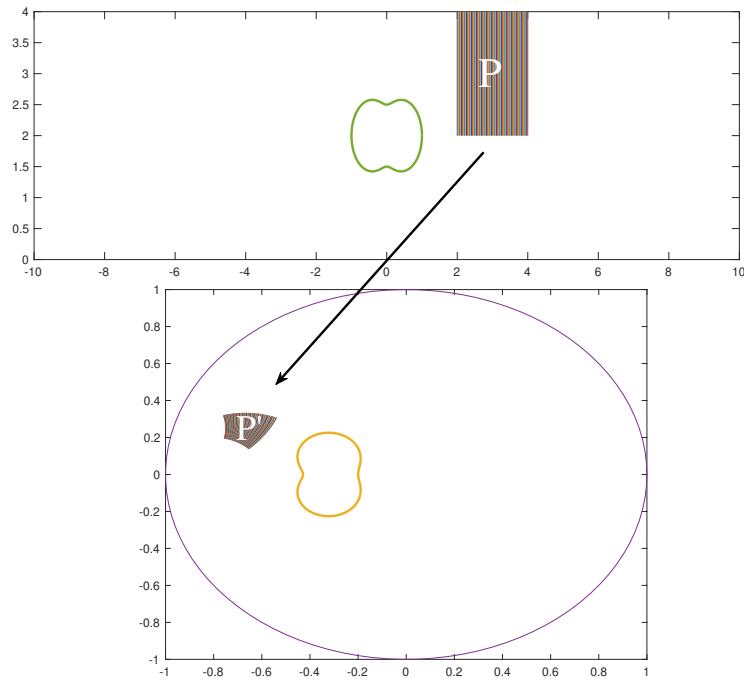
38

Figure 6.2. Transformation of a Region

6.3. Numerical Examples for the Problems Defined on the Horizontal Semi-infinite Strips

In this section, we illustrate our methods approximation results for Dirichlet and Mixed Problems on Horizontal Semi-infinite Strips with a peanut-shaped hole, see Figures 2.5 and 2.7. The numerical solution with 256 quadrature points is considered as our exact solution to evaluate error and order of convergence. Since the maps (2.5), (2.7) are more complicated than (2.2), they don't have simplified forms like (2.13). Therefore, in this section we evaluate the boundary values by using MATLAB. Additionally, visualizations for the transformations of the boundary conditions are given in this section.

6.3.1. Horizontal Semi-infinite Strip

Before we begin to solve our numerical examples, we would like to introduce you the travel of our test point for the conformal map in equation (2.5) used in this section for

Table 6.7. Infinity error norm of a specified region

n	$\|Error\|_\infty$ for (6.1)-(6.3)	$\|Error\|_\infty$ for (6.4)-(6.6)
32	0.0362	0.0362
64	6.3174×10^{-4}	6.2174×10^{-4}
128	6.1268×10^{-7}	6.1268×10^{-7}
256	2.2572×10^{-13}	2.2487×10^{-13}
512	4.4563×10^{-15}	4.0318×10^{-15}

a better understanding of the concept. Green point in Figure 6.3 represents our test point.
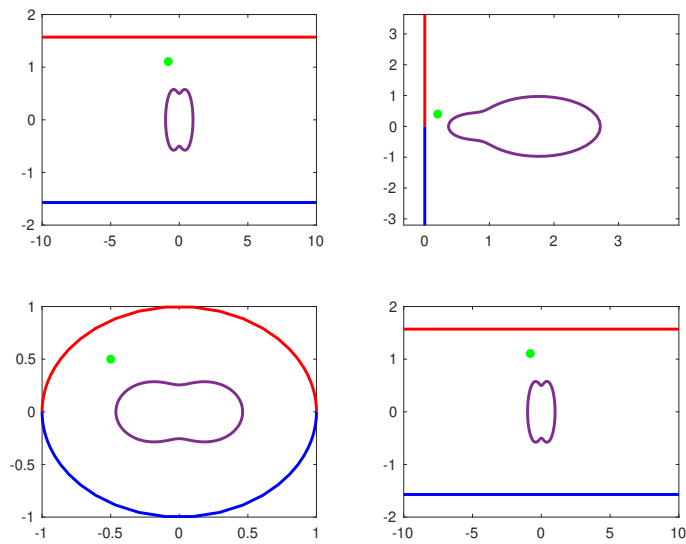

Figure 6.3. Journey of the test point for map (2.5)

Example 6.8 (Dirichlet Problem) *We try to get the solution to the problem that involves finding a function that satisfies the following boundary conditions and the Laplace Equation within the original domain(2.5, left),*

$$\Delta u = 0 \ \ in \ \ D$$

$$u(x) = 0 \ \ on \ \ \Gamma_0$$

$$u(x) = e^{-(x-1)^2} \cos 2x \ \ on \ \ \Gamma_1$$

Using the map (2.5), we transform the problem from unbounded domain to a bounded domain, we can write our transformed problem as,

$$\Delta U = 0 \ \ in \ \ D'$$

$$U(\theta) = 0 \ \ on \ \ \Gamma_0'$$

$$U(\theta) = F(\theta) \ \ on \ \ \Gamma_1'$$

In figure 6.4 you may see graphs of boundary conditions with and without treatment.

Figure 6.4 shows that the round-off error during conformal mapping from the strip to half-plane spoils the boundary conditions reflection on the new domain.
In Table 6.8 we illustrate error results of the horizontal strip conformal mapping from subsection 2.2.1, after treatment.

Table 6.8. Results are evaluated at the test point given in Figure 6.3

n	$\tilde{u}$	$Error$	$Order$	$Condition\ Number$
8	0.12166	1.3794×10^{-5}	-	18.744
16	0.12165	1.7835×10^{-7}	6.2730	18.776
32	0.12165	1.7835×10^{-11}	13.3217	18.776
64	0.12165	4.1633×10^{-17}	18.6746	18.776

Example 6.9 (Mixed Problem) *We try to get the solution to the problem that involves finding a function that satisfies the following boundary conditions and the Laplace Equa-*
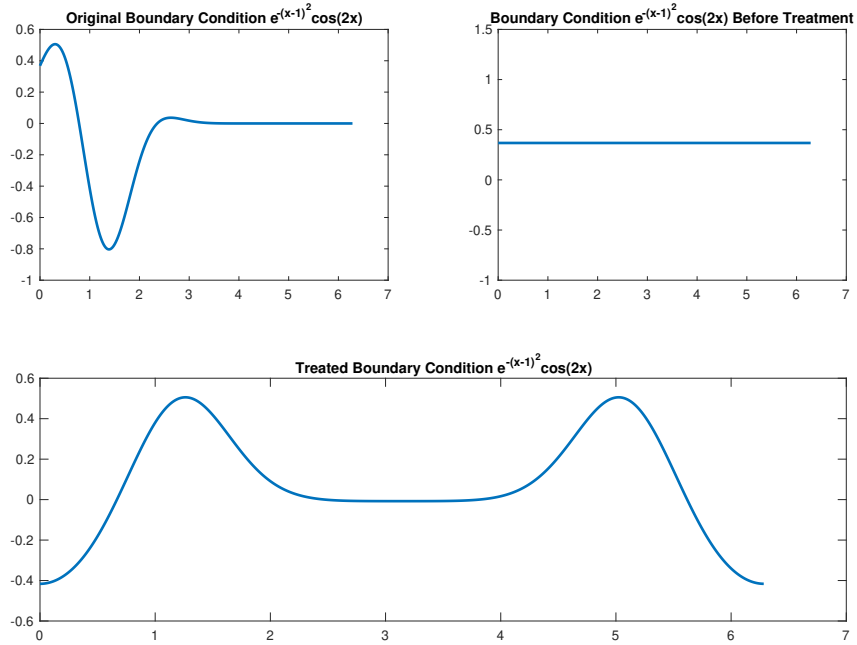
Figure 6.4. Change of Boundary Condition for Problem 6.8

tion within the original domain(2.5, left),

$$\Delta u = 0 \ \ in \ \ D$$

$$\frac{\partial u}{\partial \nu}(x) = 0 \ \ on \ \ \Gamma_0$$

$$u(x) = e^{-x^2} \ \ on \ \ \Gamma_1$$

Using the map (2.5), we transform the problem from unbounded domain to a bounded domain, we can write our transformed problem as,

$$\Delta U = 0 \ \ in \ \ D'$$

$$\frac{\partial U}{\partial \nu}(\theta) = 0 \ \ on \ \ \Gamma'_0$$

$$U(\theta) = F(\theta) \ \ on \ \ \Gamma'_1$$

In Table 6.9 we illustrate error results of the horizontal strip conformal mapping from

subsection 2.2.1, after treatment.

Table 6.9. Results are evaluated at the test point given in Figure 6.3

n	$\tilde{u}$	Error	Order of Convergence	Condition Number
8	0.63548	0.0018369	-	3.4473
16	0.63365	7.6237×10^{-6}	7.9125	3.4437
32	0.63364	2.9331×10^{-10}	14.6658	3.4438
64	0.63364	8.8818×10^{-16}	18.3332	3.4438

6.3.2. Horizontal Semi-infinite Half-Strip

In figure 6.5, you may see which path our test point follows during conformal mapping. Again, green point in Figure 6.5 represents our test point.
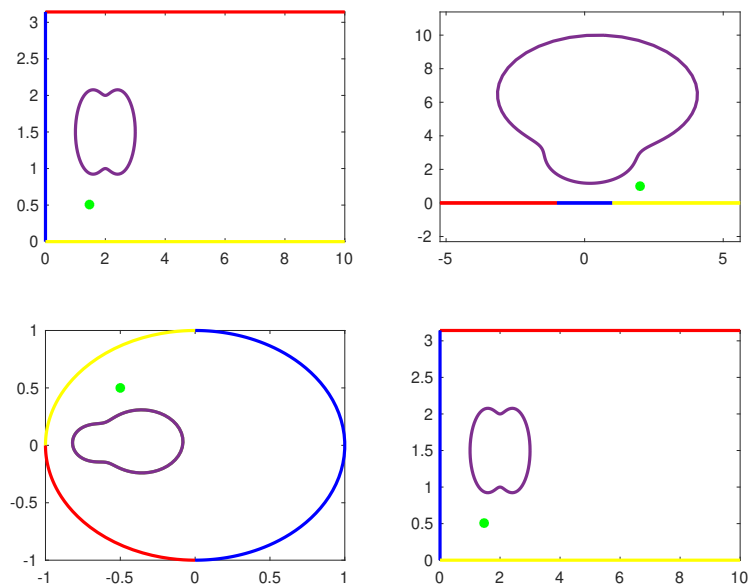

Figure 6.5. Journey of the test point for map (2.7)

Example 6.10 (Dirichlet Problem) *We try to get the solution to the problem that involves finding a function that satisfies the following boundary conditions and the Laplace*

Equation within the original domain (2.8, left),

$$\Delta u = 0 \ \ in \ \ D$$

$$u(x) = 0 \ \ on \ \ \Gamma_0$$

$$u(x) = e^{-x^2} \ \ on \ \ \Gamma_1$$

Using the map (2.7), we transform the problem from unbounded domain to a bounded domain, we can write our transformed problem as,

$$\Delta U = 0 \ \ in \ \ D'$$

$$U(\theta) = 0 \ \ on \ \ \Gamma'_0$$

$$U(\theta) = F(\theta) \ \ on \ \ \Gamma'_1$$

In Table 6.10 we illustrate error results of the horizontal half-strip conformal mapping from subsection 2.2.2, after treatment.

Table 6.10. Results are evaluated at the test point given in Figure 6.5

n	$\tilde{u}$	$Error$	$Order$	*Condition Number*
8	0.057167	0.0034	-	16.506
16	0.060681	2.5208×10^{-5}	7.1989	16.269
32	0.060656	1.243×10^{-9}	14.3071	16.269
64	0.060656	5.4817×10^{-16}	21.1127	16.269

Example 6.11 (Mixed Problem) *Now, let us consider more complex boundary conditions. This time, we set the boundary condition on Γ_0 as a function instead of a constant. We try this because we want to see the results for more realistic cases.*

We try to get the solution to the problem that involves finding a function that satisfies the following boundary conditions and the Laplace Equation within the original domain (2.8,

left),

$$\Delta u = 0 \ \ in \ \ D$$

$$\frac{\partial u}{\partial \nu}(x, y) = e^{-2x} \cos 3y \ \ on \ \ \Gamma_0$$

$$u(x, y) = \frac{e^{-y^2}}{x^2 + 1} \ \ on \ \ \Gamma_1$$

Using the map (2.7), we transform the problem from unbounded domain to a bounded domain, we can write our transformed problem as,

$$\Delta U = 0 \ \ in \ \ D'$$

$$\frac{\partial U}{\partial \nu}(\theta) = F(\theta) \ \ on \ \ \Gamma_0'$$

$$U(\theta) = G(\theta) \ \ on \ \ \Gamma_1'$$

In Table 6.11 we illustrate error results of the horizontal half-strip conformal mapping from subsection 2.2.2, after treatment.

Table 6.11. Results are evaluated at the test point given in Figure 6.5

n	$\tilde{u}$	$Error$	$Order$	$Condition \ Number$
8	-0.23857	0.28409	-	59.546
16	-0.33175	0.00449	5.9824	35.004
32	-0.33324	3.393×10^{-7}	13.6929	33.854
64	-0.33324	3.6647×10^{-15}	26.4643	33.854

6.4. Numerical Examples for the Problems Defined on the Vertical Semi-infinite Half-Strip

In this section, we illustrate our methods approximation results for Dirichlet and Mixed Problems on Vertical Semi-infinite Half-Strip with a peanut-shaped hole, see Figure 2.11. The numerical solution with 256 quadrature points is considered as our exact

solution to evaluate error and order of convergence. Since the map 2.5 is more compli-
cated than 2.2, again, it doesn't have a simplified form like (2.13). Therefore, in this
section we evaluate the boundary values by using MATLAB. Additionally, visualizations
for the transformations of the boundary conditions are given in this section.

Now, before beginning with the numerical examples, we will again visualize the journey
of our test point from the original domain to unit circle. Green point of Figure 6.6 repre-
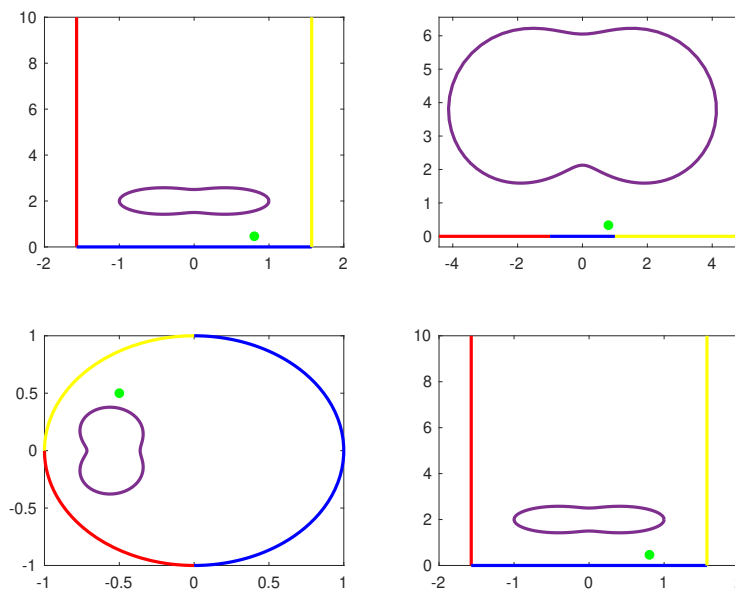sents our test point.

Figure 6.6. Journey of the test point for map (2.9)

Example 6.12 (Dirichlet Problem) *Now, let us consider more complex boundary condi-
tions. This time, we set the boundary condition on* Γ_0 *as a function instead of a constant.
The reason we try this to see the results for more realistic cases.*

*We try to get the solution to the problem that involves finding a function that satisfies the
following boundary conditions and the Laplace Equation within the original domain (2.9,*

left),

$$\Delta u = 0 \ \ in \ \ D$$

$$u(x,y) = e^{-2x}\cos 3y \ \ on \ \ \Gamma_0$$

$$u(x,y) = 5\sin(\pi x)\cos(\pi y) \ \ on \ \ \Gamma_1$$

Using the map (2.9), we transform the problem from unbounded domain to a bounded domain, we can write our transformed problem as,

$$\Delta U = 0 \ \ in \ \ D'$$

$$U(\theta) = F(\theta) \ \ on \ \ \Gamma'_0$$

$$U(\theta) = G(\theta) \ \ on \ \ \Gamma'_1$$

In Table 6.12 we illustrate error results of the horizontal strip conformal mapping from subsection 2.2.3, after treatment.

Table 6.12. Results are evaluated at the test point given in Figure 6.6

n	$\tilde{u}$	$Error$	$Order$	*Condition Number*
8	-0.88224	0.034228	-	84.214
16	-0.909	0.0082154	3.7394	94.4
32	-0.91647	1.1976×10^{-6}	1.2114	93.121
64	-0.91647	1.0474×10^{-11}	12.7322	93.12
128	-0.91647	1.2114×10^{-15}	16.8030	93.12

Example 6.13 (Mixed Problem) *We try to get the solution to the problem that involves finding a function that satisfies the following boundary conditions and the Laplace Equation within the original domain (2.9, left),*

$$\Delta u = 0 \ \ in \ \ D$$

$$\frac{\partial u}{\partial \nu}(x) = 0 \ \ on \ \ \Gamma_0$$

$$u(x) = e^{-x^2} \ \ on \ \ \Gamma_1$$

Using the map (2.9), we transform the problem from unbounded domain to a bounded domain, we can write our transformed problem as,

$$\Delta U = 0 \;\; in \;\; D'$$

$$\frac{\partial U}{\partial \nu}(\theta) = 0 \;\; on \;\; \Gamma_0'$$

$$U(\theta) = F(\theta) \;\; on \;\; \Gamma_1'$$

Table 6.13. Results are evaluated at the test point given in Figure 6.6

n	$\tilde{u}$	*Error*	*Order of Convergence*	*Condition Number*
8	0.56102	0.0164	-	55.761
16	0.54459	7.0822×10^{-5}	7.8517	44.063
32	0.54466	6.213×10^{-10}	16.7985	43.911
64	0.54466	1.5543×10^{-15}	18.6087	43.911

Figure 6.7 shows that the round-off error during conformal mapping from the strip to half-plane spoils the boundary conditions reflection on the new domain.
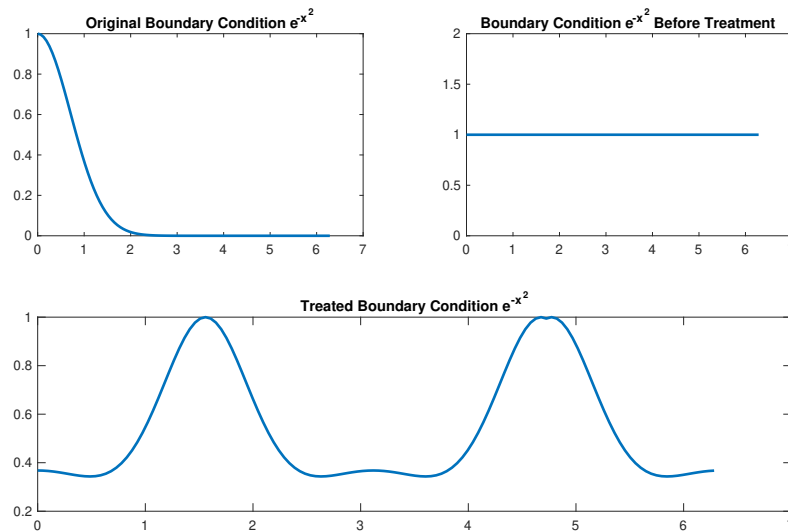

Figure 6.7. Change of Boundary Condition for Problem 6.12

6.5. Further Numerical Examples

In this section, we will give examples of the real-life applications of Laplace Boundary Value Problems subject to Dirichlet and Mixed boundary conditions on semi-infinite domains. Afterward, we will solve the problems with the method proposed and visualize the solutions in the original domain. The aim of this section is to show applicability of the method in engineering problems.

Example 6.14 *Let us consider our domain in Figure 2.9, a semi-infinite strip representing a thin conducting plate with a peanut-shaped hole. The plate is made of a conductive material, and we are interested in studying the temperature distribution on a specified region of the plate. The boundary conditions of this problem can be specified as follows,*

$$\Delta u = 0 \ \ in \ \ D$$

$$u(x, y) = 0 \ \ on \ \ \Gamma_0$$

$$u(x, y) = \frac{e^{-x^2}}{y^2 + 1} \ \ on \ \ \Gamma_1$$

The aim of this boundary value problem is to discover the temperature distribution, inside the semi-infinite strip. Therefore, we transform our problem to the unit circle by using conformal map (2.9). We result with the following problem,

$$\Delta U = 0 \ \ in \ \ D'$$

$$U(\theta) = 0 \ \ on \ \ \Gamma'_0$$

$$U(\theta) = F(\theta) \ \ on \ \ \Gamma'_1$$

Now the next step to solve the problem is to mesh a region on the plate and map that region to the unit circle.

One can see the journey of our solution from unit circle to original domain in Figure 6.9
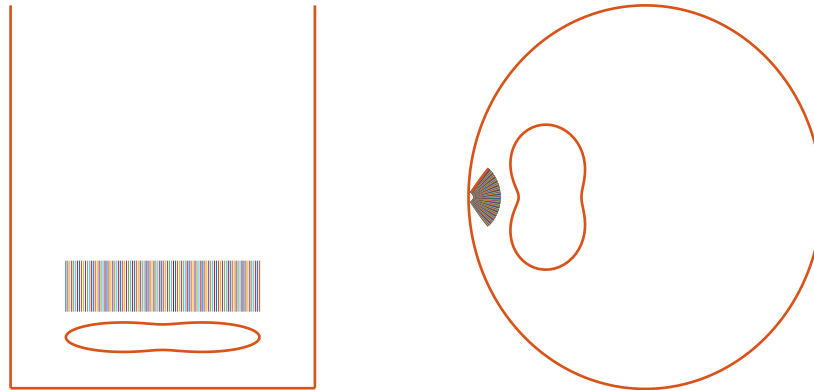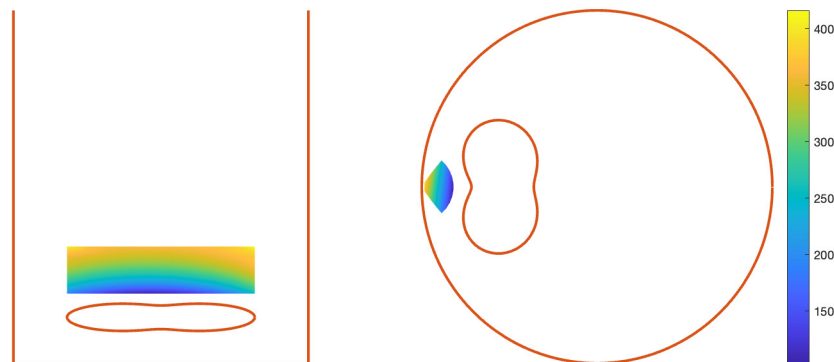
Figure 6.8. Conformal Mapping of a specified region

Figure 6.9. Solution in the original domain

Example 6.15 *Now we consider a two-dimensional semi-infinite horizontal strip representing a flow channel with a peanut-shaped obstruction, like reduced flow velocity, see Figure 2.5. We may define the boundary conditions as follows,*

$$\Delta u = 0 \ \ in \ \ D$$

$$\frac{\partial u}{\partial \nu}(x, y) = 0 \ \ on \ \ \Gamma_0$$

$$u(x, y) = e^{-3x^2} \cos 2y \ \ on \ \ \Gamma_1$$

To solve this boundary value problem, we use conformal map (2.5) to the unit circle, and

we result with the following boundary conditions,

$$\Delta U = 0 \ \ in \ \ D'$$

$$\frac{\partial U}{\partial \nu}(\theta) = 0 \ \ on \ \ \Gamma_0'$$

$$U(\theta) = F(\theta) \ \ on \ \ \Gamma_1'$$

Now let us specify a region and map it to the unit circle, and after solving the problem we
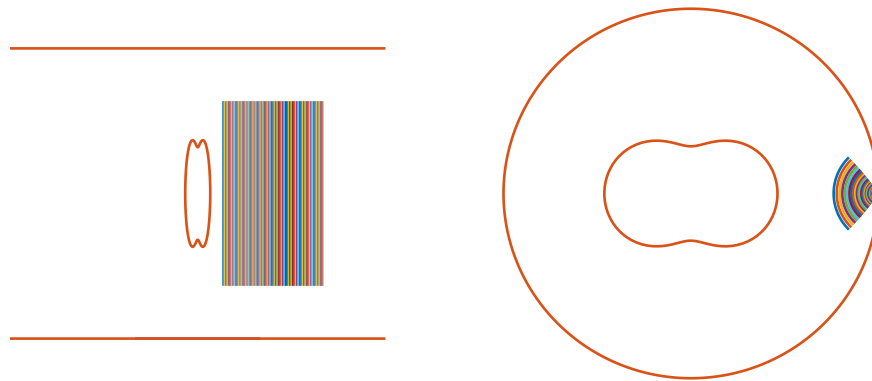

Figure 6.10. Conformal mapping of a specified region

go back to the original domain as follows,

Figure 6.11. Solution in the original domain

Example 6.16 *We consider the problem 6.14, but this time we will try to find the infinity norm of the error on a line and a region. The reason we choose to take the points on 6.12 is to see the methods accuracy near infinity. Because we sent $-\infty$ and ∞ to $(-1, 0)$ via conformal mapping (2.9) and the infinity error norm of the solution on the region closer to that point should give a closer value to the maximum error possible. The Table 6.14 presents the results of the infinity error calculations.*
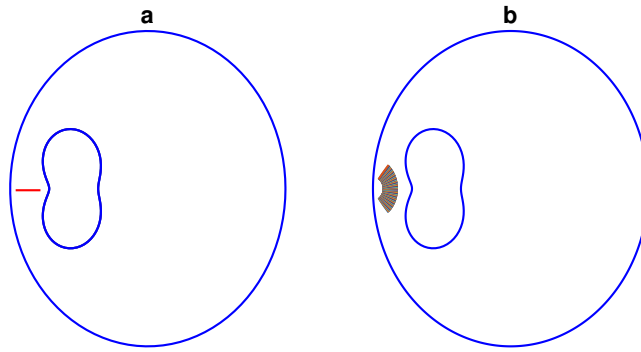

Figure 6.12. Mapped (a) Line and (b) Region on the Unit Circle

Table 6.14. Infinity Error Norm of a Line

n	$\|Error\|_\infty$ for Figure 6.12.(a)	$\|Error\|_\infty$ for Figure 6.12.(b)
16	0.0050	2.0340
32	1.3960×10^{-6}	0.7411
64	1.9929×10^{-14}	0.0052
128	4.2744×10^{-15}	5.4708×10^{-4}
256	6.1062×10^{-16}	2.1835×10^{-8}
512	-	1.6431×10^{-14}

It can be seen from the Table 6.14 that our method converges effectively for larger values of n. This is primarily due to the fact that the solution exhibits considerable magnitudes at infinity. As a result, we can conclude that our approach consistently produces satisfactory results, even when dealing with the solution close to infinity.

CHAPTER 7

CONCLUSION

In this thesis, boundary value problems for Laplace Equation are solved in doubly connected semi-infinite domains by using boundary integral equations. The semi-infinite domains are mapped to the unit circle with the aid of conformal maps, and images of the boundary conditions are evaluated. The reliability of conformal maps which includes the composition of functions is investigated to avoid round-off errors. The mapping errors were treated by rewriting the conformal maps in different forms and evaluating them by hand in the problematic points. Besides, changes in the boundary conditions after conformal mappings are illustrated with graphs. Afterward, solution representations via using boundary integral equations to the Dirichlet and Mixed boundary value problems are constructed. After imposing the boundary conditions, they lead us to systems of Fredholm integral equations of the second kind. The existence of unique solutions to the systems of boundary integral equations is proved. In the case of Dirichlet boundary conditions, a new modification on the double-layer potential was introduced to ensure the unique solvability of the system. Nonetheless, in the case of mixed boundary conditions, such modification was not needed. The numerical solutions of the constructed systems of boundary integral equations Nyström Method based on the trapezoidal rule was used. For the integral operators with weakly singular kernels, a method based on splitting off the singularity is used. To calculate the singular parts of the integrals, we used a special quadrature rule which is based on trigonometric interpolation. Numerical examples exhibited that for analytic and sufficiently smooth boundary conditions our method converged exponentially for the solutions of the Dirichlet and Mixed problems on doubly connected semi-infinite domains. It is validated by the numerical examples that the proposed numerical method super-algebraically converged, as expected. As a result, the method we used has been exhibited to be effective for the Dirichlet and Mixed boundary value problems for the Laplace boundary value problems on semi-infinite domains.

REFERENCES

[1] O. M. FALTINSEN and Y. A. SEMENOV, "The effect of gravity and cavitation on a hydrofoil near the free surface," *Journal of Fluid Mechanics*, vol. 597, p. 371–394, 2008.

[2] U. K. De and A. K. Raychaudhuri, "Static distribution of charged dust in general relativity," *Proceedings of the Royal Society of London. Series A, Mathematical and Physical Sciences*, vol. 303, no. 1472, pp. 97–101, 1968. [Online]. Available: http://www.jstor.org/stable/2415867

[3] M. A. Gottlieb and R. Pfeiffer, *Electrostatic Analogs by Richard Feynman, Ch12-S5*.

[4] J. Saleh, *Fluid Flow Handbook*, ser. McGraw-Hill handbooks. McGraw-Hill Companies,Incorporated, 2002. [Online]. Available: https://books.google.com.tr/books?id=4CFxR7CKA-8C

[5] M. XUE, H. XÜ, Y. LIU, and D. K. P. YUE, "Computations of fully nonlinear three-dimensional wave–wave and wave–body interactions. part 1. dynamics of steep three-dimensional waves," *Journal of Fluid Mechanics*, vol. 438, p. 11–39, 2001.

[6] Y. LIU, M. XUE, and D. K. P. YUE, "Computations of fully nonlinear three-dimensional wave–wave and wave–body interactions. part 2. nonlinear waves and forces on a body," *Journal of Fluid Mechanics*, vol. 438, p. 41–66, 2001.

[7] Y. Liu, *Fast Multipole Boundary Element Method: Theory and Applications in Engineering*. Cambridge University Press, 2009.

[8] G. Xu and G. Wu, "Boundary element simulation of inviscid flow around an oscillatory foil with vortex sheet," *Engineering Analysis with Boundary Elements*, vol. 37, no. 5, pp. 825–835, 2013. [Online]. Available: https://www.sciencedirect.com/science/article/pii/S0955799713000489

[9] K. Erhard, "Point source approximation methods in inverse obstacle reconstruction problems," Ph.D. dissertation, Göttingen, Univ., Diss., 2005, 2005.

[10] O. H. Menin, V. Rolnik, and A. S. Martinez, "Boundary element method and simulated annealing algorithm applied to electrical impedance tomography image reconstruction," *Revista Brasileira de Ensino de Física*, vol. 35, 2013.

[11] P. N. Ivanshin and E. A. Shirokova, "The solution of a mixed boundary value problem for the laplace equation in a multiply connected domain," *Probleme Analiza*, vol. 8, no. 2, pp. 51–66, 2019.

[12] W. Mclean, *Strongly elliptic systems and boundary integral equations*. Cambridge University Press, 2000.

[13] "Möbius transformation is bijection." [Online]. Available: https://proofwiki.org/wiki/Möbius_Transformation_is_Bijection

[14] P. J. Olver, *Complex analysis and conformal mapping*. University of Minnesota 806, 2017.

[15] N. Asmar and L. Grafakos, *Complex Analysis with Applications*, ser. Undergraduate Texts in Mathematics. Springer International Publishing, 2018. [Online]. Available: https://books.google.com.tr/books?id=HXFyDwAAQBAJ

[16] W. A. AYAD, O. I. ELHASADI, Z. A. KHALLEEFAH, and A. A. AHMED, "Conformal mapping as a tool in solving some mathematical and physical problems."

[17] R. Kress, *Linear integral equations*. Springer, 2014, vol. 82.

[18] K. Atkinson and W. Han, *Elementary Numerical Analysis*. Wiley, 2004. [Online]. Available: https://books.google.com.tr/books?id=F_4gPwAACAAJ

[19] O. I. Yaman and G. Özdemir, "Numerical solution of a generalized boundary value problem for the modified helmholtz equation in two dimensions," *Mathematics and Computers in Simulation*, vol. 190, pp. 181–191, 2021.

[20] R. Chapko and B. Johansson, "An alternating potential-based approach to the cauchy problem for the laplace equation in a planar domain with a cut," *Computational Methods in Applied Mathematics*, vol. 8, no. 4, pp. 315–335, 2008.

[21] R.   Kress,   *Numerical Analysis*,   ser.   Graduate   Texts   in   Math-
       ematics.   Springer   New   York,   2012.   [Online].   Available:
       https://books.google.com.tr/books?id=Jv_ZBwAAQBAJ

[22] E. Brew, *An introduction to numerical analysis, by Kendall E. Atkinson. Pp xiii, 587.£
       12· 55. 1978. SBN 0 471 02985 8 (Wiley).*   Cambridge University Press, 1979,
       vol. 63, no. 425.